RAPID SEISMIC SCREENING OF REINFORCED CONCRETE BUILDINGS
USING ENERGY-BASED PRINCIPLES

by

Ahmet Mehdi Darılmaz

B.S., Civil Engineering, Boğaziçi University, 2018

Submitted to the Institute for Graduate Studies in

Science and Engineering in partial fulfillment of

the requirements for the degree of

Master of Science

Graduate Program in Civil Engineering

Boğaziçi University

2022

ACKNOWLEDGEMENTS

I would like to express my sincere gratitude to my thesis supervisor Prof. Cem Yalçın for his guidance and never-ending patience throughout my studies. I could not have undertaken this journey without his guidance and encouragement.

I would like to extend my sincere thanks to Prof. Kutay Orakçal and Prof. Oğuz Cem Çelik for serving as members of my thesis committee and providing their valuable suggestions for this study's improvement.

I would like to express my deepest appreciation to Selahattin Akalp and Burak Horoz for their incredible assistance and friendly encouragement throughout my thesis work. Their collaborative approach has been a great source of motivation.

Words cannot begin to express my gratitude to my dear wife, Feyza Köseoğlu Darılmaz for her unconditional love, support, and encouragement throughout my graduate studies.

Last but not least, I would like to thank my beautiful daughter Zeynep Ela for being my muse during the challenging last few months of my studies.

ABSTRACT

RAPID SEISMIC SCREENING OF REINFORCED CONCRETE BUILDINGS USING ENERGY-BASED PRINCIPLES

Seismic evaluation methods were developed and employed in seismic design codes for the purpose of avoiding life loss in the aftermath of earthquakes. The high death and economic toll from previous earthquakes highlight the importance of this evaluation for the residential structures in Turkey. However, the task of evaluation is challenging due to the abundance of structurally flawed buildings. Therefore, use of quick screening techniques is essential. Current rapid screening methods rely either on force or displacement-based approaches, which fail to employ some important parameters of earthquakes such as earthquake duration, frequency content, and energy dissipation capacity. Another approach which has been under development since the 1980s, the energy-based approach, was proven to be more successful in employing these parameters. Thus, the aim of this study is to develop a rapid seismic screening method for residential reinforced concrete structures that employs energy-based principles and evaluates the performance using the guidelines of the Turkish Seismic Code. A MAT-LAB program, which executes a modified version of the energy-based design algorithm proposed by Yalçın *et al.* [1], was developed to conduct a parametric study related to the parameters determining the earthquake energy demand and energy dissipation capacity of structures. Additional parameters related to structural irregularities and deficiencies were also employed in this study. The results of the parametric study were subjected to statistical analyses to produce a simple model for estimating the damage score of the structures under various scenarios, which in turn was used to predict the performance level of the structures.

ÖZET

BETONARME BİNALARIN ENERJİ BAZLI PRENSİPLERLE HIZLI SİSMİK DEĞERLENDİRİLMESİ

Sismik değerlendirme metotları deprem sonrası can kaybını minimize etmek için geliştirilmiş ve yönetmeliklere dahil edilmiştir. Eski depremlerde gözlemlenen yüksek can ve mal kayıpları sismik değerlendirme sürecinin Türkiye'deki konut yapıları için önemini göstermektedir. Ancak, yapısal olarak kusurlu bina sayısının çokluğu bu değerlendirme sürecini zorlaştırmaktadır. Bu nedenle, hızlı değerlendirme tekniklerinin kullanılması gereklidir. Mevcut hızlı tarama yöntemleri, deprem süresi, frekans içeriği ve enerji dağılım kapasitesi gibi bazı önemli deprem parametrelerini kullanmayan kuvvet veya yer değiştirmeye dayalı yaklaşımlara dayanmaktadır. 1980'lerden beri geliştirilen enerji bazlı tasarım metotlarının bu parametreleri kullanmada daha başarılı olduğu kanıtlanmıştır.

Bu çalışmanın amacı, konut tipi betonarme yapılar için enerji bazlı prensipleri kullanan ve Türk Deprem Yönetmeliği ilkelerince yapıların performansını değerlendiren bir hızlı sismik tarama yöntemi geliştirmektir. Yalçın ve diğerleri [1] tarafından önerilen, enerji bazlı tasarım algoritmasının değiştirilmiş bir versiyonunu yürüten bir MAT-LAB programı, yapıların deprem enerji talebini ve enerji yutma kapasitesini belirleyen parametreleri inceleyen parametrik bir çalışma yapmak için geliştirilmiştir. Yapısal düzensizliklerle ilgili ek parametreler de bu çalışmaya dahil edilmiştir. Parametrik çalışmanın sonuçları, çeşitli senaryolar altında yapıların hasar skorunu tahmin eden bir model üretmek amacıyla istatistiksel analizlere tabi tutulmuştur. Bu model de yapıların performans düzeylerini tahmin etmek için kullanılmıştır.

TABLE OF CONTENTS

LIST OF FIGURES

LIST OF TABLES

LIST OF SYMBOLS

c	Damping Coefficient
E_a	Absorbed Energy
E_d	Damping Energy
E_k	Kinetic Energy
E_I	Input Energy
E_p	Plastic Strain Energy
E_s	Elastic Strain Energy
f_s	Spring Force
k	Stiffness
m	Mass
R	Force Reduction Factor
μ	Ductility
ρ	Reinforcement Ratio

LIST OF ACRONYMS/ABBREVIATIONS

2D	Two Dimensional
3D	Three Dimensional
API	Application Programming Interface
AFAD	Disaster and Emergency Management Presidency
ASCE	American Society of Civil Engineers
EBD	Energy-Based Design
EPP	Elastic-Perfectly-Plastic
MDOF	Multi Degree of Freedom
OLS	Ordinary Least Squares
PGA	Peak Ground Acceleration
RC	Reinforced Concrete
SDOF	Single Degree of Freedom
TSC	Turkish Seismic Code

1. INTRODUCTION

1.1. General

One of the main objectives of structural engineers is to reduce the harmful and life-threatening impacts of earthquakes. Understanding the nature of earthquakes and how they damage structures is the key to averting such consequences, whether for the design of new buildings or for assessing the state of existing ones.

Numerous earthquakes with significant fatality rates, including the 1999 Düzce, 1999 Kocaeli, and 2011 Van earthquakes, revealed Turkey's lack of comprehension and poor construction techniques for earthquake-resistant buildings. Consequently, throughout the past three decades, new seismic design rules were implemented and improved design methods are now being applied to new structures. Nevertheless, the status of the existing ones remains unaffected and assessing their performance levels, retrofitting if necessary, is imperative for avoiding financial and human losses.

Analyzing the vast number of at-risk structures using traditional procedures defined in seismic codes is a time-consuming and expensive task. The same is true for establishing the strengthening or seismic retrofitting method for each single building, as well as reanalyzing those that have previously been retrofitted. This is why the use of quick screening processes is vital. There are numerous approaches in the literature that attempt to create such procedures, some of which are discussed in the following subsections. The majority of them employ visual evaluation techniques, while others base their work on numerical and experimental studies. Those that construct the basis of their screening processes using numerical analytic methods profit from either Force-Based or Displacement-Based approaches. These techniques are used in the field and are well accepted. However, they have a number of drawbacks that may be resolved by utilizing the principles of Energy-Based Design.

This study explores the structural deficiencies present in existing typical residential buildings in Turkey and aims to develop a quick seismic screening procedure which will comply with the requirements of Turkish Seismic Code by using the Energy-Based Design principles as a foundation.

1.2. Current Design Approaches

The two most widely used design approaches, namely Displacement-Based and Force-Based, are discussed in the following subsections. Their strengths and weaknesses are emphasized.

1.2.1. Force-Based Approach

Due to its ease of use and speed of computations, the Force-Based design approach has been one of the most popular approaches for seismic design. Through approximating elastic behavior, it aims to model the inelastic behavior of structures under dynamic loads. In this process, inclusion of the dynamic characteristics of the structure and soil-structure interaction is essential.

The primary concept behind this method is to use the structures' elastic properties to calculate their inelastic response to the strongest forces that may possibly be applied to them. Through the use of Elastic Response Spectra, which use Peak Ground Acceleration (PGA), soil type, and damping ratio as main parameters, the elastic demand is estimated. Calculating the dominant natural period of the structure is sufficient to obtain the earthquake demand from these spectra. Therefore, it's crucial that structural members' preliminary design is done well and this requires great expertise.

Having found the maximum earthquake demand, as a next step, inelastic deformation capacity is required to be calculated. The Force Reduction Factor R was found by researchers to be a great indicator for these calculations. It was also found

that R is a function of displacement ductility capacity μ [2, 3]. Benefiting from the relationship between these two, equal displacement and equal area (energy) approximations are made to calculate the lateral load capacity of the structure . Figure 1.1 depicts these approximations. Equal displacement approximation is used for long period structures whereas equal area approximation is used for short period structures. The force reduction factor R is considered to be equal to displacement ductility in equal displacement approximation while it is less than displacement ductility in equal area approximation [4, 5].

(a) Equal Displacement.   (b) Equal Area.
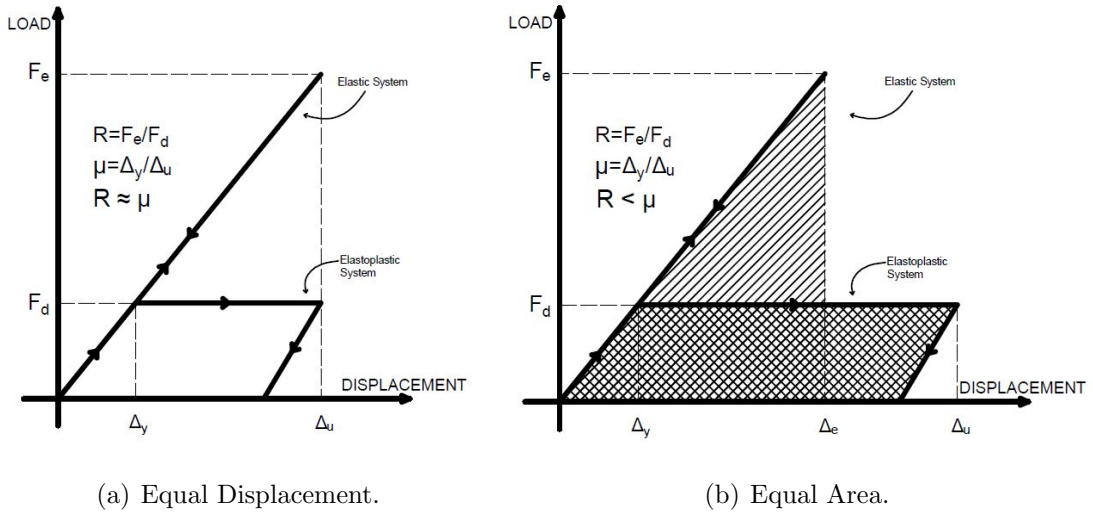
Figure 1.1. Equal Displacement and Equal Area Approximations.

This approach has been adopted and modified numerous times by seismic design codes, however it has some limitations. Since they directly affect the dynamic characteristics, it necessitates an intensive and iterative procedure where the dimensions of the structural components are continuously updated. Focusing solely on the peak response, either in terms of velocity or acceleration, omits the effect of structure's performance and the hysteretic energy dissipation capacity. Consequently, the structure's accumulating damage is neglected [6]. Since the total damage reflects the characteristics and duration of earthquakes, which is very significant.

Another downside of this approach is that there is no agreement in the literature as to how to find the yield and ultimate displacements, which characterize the behavior of the structure. Additionally, it is presumed that the structure would respond in an elasto-plastic way, disregarding its hysteretic properties [2].

1.2.2. Displacement-Based Approach

With the understanding that a structure's vulnerability is better described by the displacements it could withstand under dynamic loads, the paradigm of earthquake engineering shifted from Strength-Based Design to Displacement-Based Design in the 1980s and 1990s [7]. As a result, the development of new design methodologies that employ this strategy had begun. These techniques favor a structure's performance over its strength, suggesting that strength is only important for endurance against displacements.

A method that adopts this approach was proposed by Priestley and Calvi [8]. This method has applications both for Single-Degree-of-Freedom (SDOF) and Multi-Degree-of-Freedom (MDOF) systems. The process is initiated with a preliminary design and the estimation of the structural yield and ultimate displacement levels. The utilization of a pushover analysis is required at this stage. Using the results of this analysis, force-displacement graphs (capacity curves) are constructed. Meanwhile, using the stiffness calculated at preliminary design, response spectra are constructed. By the combination of these two types of curves, target displacements are acquired. The relationship between the target and yield displacement reflects the ductility, which is a design criteria. An iterative process is repeated until the desired displacement capacity set by the engineer is reached.

While there are great advancements in the understanding of structural performance thanks to this method, it has some inadequacies. Even though this approach better captures the performance and capacity of the structure, on the demand side it still relies on elastic design spectra. Similar to Force-Based Approach, this method

works at structure level, by focusing on the relationship between top displacement and base shear, and is unable to evaluate the performance on the member level. Last but not least, it fails to include the frequency content and duration of earthquakes. Therefore, total cumulative damage is still neglected [9].

1.3. Energy-Based Approach

Considering the common shortcomings of strength and performance focused design methodologies, it could be concluded that the earthquake resistant design processes need to include the energy dissipation capacity of as a parameter which occurs in the form of damping and plastic strain energy. By employing earthquake duration, frequency content, and energy dissipation capacity as factors, the Energy-Based approach differentiates from previous approaches.
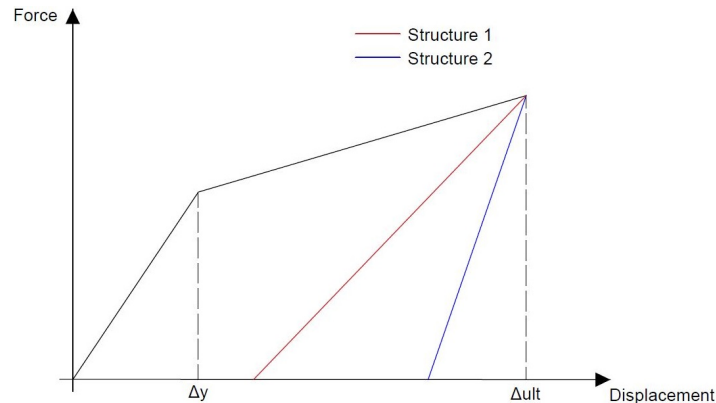
Figure 1.2. Two identical structures with different energy dissipation capacities.

Chopra [6] made the suggestion that the energy dissipated by a structural member could be calculated from the area under the force-displacement curve. Hence, in addition to the loading phase, the unloading phase is crucial for determining the capacity which is disregarded by Displacement-Based approaches. Figure 1.2 depicts two identical structures in regards to their similar backbone curves, but different behavior models [9]. These structures perform very differently under cyclic loads, and their total dissipated energy values differ from one another.

Development of Energy-Based seismic design methods goes back to the proposal made by Housner [10]. His method used the earthquake duration and frequency content for structural damage calculation. Following his study, many researchers worked more on this topic.

The main parameters, according to Zahrah and Hall's research [11] into the causes of damage due to the ground motion in SDOF systems, are the energy absorbed and the energy dissipated by the structure. Akiyama [12] was one of the first researchers to employ energy formulations on Multi Degree of Freedom (MDOF) systems. He suggested that the hysteresis energy should be distributed uniformly to the structure whereas some other researchers [13, 14] asserted that distributing it linearly along the height is more advisable.

Ye *et al.* [15] developed a design framework where they acquired the energy demand from their input energy spectra and calculated the distribution of hysteresis energy to the members. Through an equation they created for the ratio of the two, they were able to separate the hysteresis energy from the input energy. Using this relation they determined damping levels. They validated their method by applying it on steel braced frames.

In his Ph.D. thesis, Dindar [9] investigated the energy demand and dissipation capacities of reinforced concrete columns. He also proposed a design methodology for them. On the basis of energy concepts, Dindar [16] developed Earthquake Demand Spectra. His spectra take into account variables like soil type, ductility, earthquake intensity, and the dominant period of the structure. In contrast to earlier research that only concentrate on elasto-plastic models, his Input and Plastic Energy Demand Spectra contain a mix of six different constitutive behavior models. Therefore, they are suitable for reinforced concrete structures, which is the focus of this study.

An Energy-Based design algorithm for reinforced concrete frames was put forth by Yalçın *et al.* [1] Their approach uses constant amplitude cyclic analyses for en-

ergy dissipation capacity calculations and Dindar's spectra for demand calculations. It suggests modifications in the section design based on a comparison of Demand and Capacity terms. Additionally, it obsoletes the load reduction factor R when determining the inelastic response, which is a significant improvement over the other methods. This study benefits from this algorithm for the evaluation of existing structures.

1.4. Literature Review

Earthquake performance evaluation of the existing structures is one of the most vital tasks that need to be fulfilled, especially in regions with high seismic activity. Even though contemporary seismic design codes guide engineers through designing earthquake resilient structures very well, the existing structures still must be examined considering the possible design or practice flaws resulting from their initial construction stages or even older inadequate design methods.

1.4.1. Rapid Screening Procedures

Rapid screening methodologies have been developed in order to estimate the structures' performance for the upcoming earthquakes. While some of these methods depended only on visual screening, several different criteria were put into consideration for the evaluation process by other studies. These criteria include the existence of design flaws such as torsional irregularities, vertical discontinuities and irregularities, presence of soft story, presence of short column, presence of weak story, discontinuities in plan, weight irregularities, and strong beam-weak column relationships. Structural deficiencies that affect the screening process also include lack of redundancy, poor workmanship, poor material quality, and lack of adequate detailing.

Özdemir [17] proposed a quick seismic evaluation method for existing buildings. The method is well suited for 3-9 story Reinforced Concrete residential buildings in Turkey. He examined 4 different structure types with distinct structural deficiencies by focusing on their period and drift demands. It is assumed that these structures have

slabs that are rigid diagrams and have no shear walls. The system ductility demand is assumed to be equal to the displacement ductility demand of an individual column. P-delta effects were included in the demand analyses. He proposed a formulation for calculating the period values where 3D analysis results were utilized. Story drift demands were calculated by 2D computer analyses, and these demands were compared with the capacity charts developed by the author. In the calculation of the ductility demand, a Displacement-Based approach was used. The ductility demand and the strength reduction factor were found to be equal and used as the main parameter when assessing a structure's performance. Therefore, his approach is a hybrid approach which considers both strength and performance as indicators.

Özcebe *et al.* [18]'s method assesses structures' performance levels by assigning them damage scores. As for the parameters that determine the damage level, they selected the number of stories (N), minimum normalized lateral stiffness index (MNLSTFI), minimum lateral strength index (MNLSI), normalized redundancy score (NRS), soft story index (SSI), and overhang ratio (OR). Due to a lack of data and in an effort to speed up the screening process, two main damage classifications were developed, namely Life Safety Performance Classification (LSPC) and Immediate Occupancy Performance Classification (IOPC). To calculate damage scores based on the aforementioned parameters and to determine cut-off values, they developed two sets of formulas. They came to the conclusion that while the number of stories (N) is the most crucial factor for both LSPC and IOPC, the normalized redundancy score (NRS) is the second-most crucial factor for IOPC. Yakut *et al.* [19] enhanced this approach by using it for various soil types and ground motion characteristics. They modified the cut-off formulae by including spectral displacement as the damage-inducing ground motion parameter.

Tezcan *et al.* [20] proposed a rapid screening method, known as the "P25 Method", which aims to evaluate the existing structures as soon as possible so that the life loss is kept at the minimum. The procedure in this method evaluates 7 basic scores (P_1 through P_7) which correspond to 7 different failure modes. Base Structural Score P_1

is calculated through the formula

$$P_1 = P_0 \left(\prod_{i=1}^{14} f_i \right), \tag{1.1}$$

where P_0 is the Structural System Score which reflects the properties of the load-bearing system such as the building height, moment of inertias, and areas of the structural members. The f_i correspond to the structural irregularity coefficients. They consist of torsional irregularities, slab discontinuity, vertical discontinuity, mass irregularity, the presence of corrosion, the presence of the mezzanine floor, weak column-strong beam, stirrup spacing, soil type, foundation type and depth, elevation difference in floors, façade element weight and concrete class. P_2 through P_7 are the short column score, the soft (or weak) story score, the frame discontinuity score, the pounding score, the liquefaction potential score, and the soil movement score, respectively. When calculating the final score of the structure, these scores are summed after being multiplied with their predetermined weighting factors with the exception of the minimum one (P_{min}) being multiplied by 4. The weighted score, which is denoted by P_w, is calculated using the weighting factors from Table 1.1 with the formulation

$$P_w = \frac{\sum (w_i * P_i)}{\sum w_i}, \tag{1.2}$$

where w_i correspond to the weighting factor for each score.

Table 1.1. P scores and their weights.

Score	P_1	P_2	P_3	P_4	P_5	P_6	P_7	P_{min}
w_i	4	1	3	2	1	3	2	4

Using P_w, α and β correction factors are calculated. Then, the final score P is found by multiplying these two and P_{min}. This final score determines the collapse risk level of the structure.

New design methodologies are being developed since some key aspects of earthquake design are disregarded in the current seismic design codes and the studies mentioned above. These include duration and the frequency content of an earthquake,

hysteretic behavior of the structure, and energy imparted on the structure. Energy-Based Design methodology inherits all these features. Therefore, it is foreseen by academic authorities that new design codes will include these methods in the near future [21]. 2018 Turkish Seismic Code [22] contains guidelines of several linear and nonlinear seismic design and evaluation methods. These methods use either Force-Based or Displacement-Based approaches. Nevertheless, there is no method related to the Energy-Based approach. Once new seismic design codes adopt Energy-Based design methods, there will be a need for updated rapid seismic screening procedures which are based on Energy-Based principles. Hence, it is aimed in this thesis to develop such a method.

1.5. Objective and Scope of the Study

This thesis focuses on developing a rapid seismic screening method for reinforced concrete structures which will comply with the Turkish Earthquake Code while incorporating Energy-Based design principles. The Energy-Based design algorithm proposed by Yalçın *et al.* [1], which includes the input demand energy and member dissipation capacity calculations of reinforced concrete structures was utilized. The scope of the parametric study is limited to 3-9 story moment resisting frames with 4 bays. Rectangular sections with concrete compressive strength varying from 8 MPa to 20 MPa and reinforcement ratio varying from 0.7% to 2% are used. A set of 2D frames reflecting the typical residential buildings in Turkey with the most common structural deficiencies such as presence of soft story, lack of adequate detailing are analyzed using the Energy-Based design algorithm. Due to the limitations of the analysis methods used in the study, some common flaws in residential structures, such as pounding and frame discontinuity, had to be excluded. 60 possible cases defining the energy demand created from different soil types, peak ground acceleration levels and ductility levels are examined for each building model. The outcomes of these analyses are investigated statistically and used as a basis for the proposed seismic screening methodology.

1.6. Research Rationale

Considering the current literature, no study that adopted Energy-Based methodology to create a rapid screening procedure has been conducted. With the utilization of the Energy-Based Design methodology proposed by Yalcin *et al.* [1], the plastic energy dissipation capacity of each member under cyclic loads, frequency content, and duration of ground motions, which were not considered in other seismic evaluation processes, were included in this study. This will improve the accuracy of the screening process.

1.7. Thesis Outline

This thesis consists of four chapters. Chapter 1 includes an overview of the present study, a literature review, and the basic concepts of various design approaches.

Chapter 2 introduces the Energy Balance Equation and the derivation of its formulations. It discusses the concepts of earthquake energy demand and energy dissipation capacity as well as how these concepts are quantified in several methods. A detailed explanation of the Energy-Based Design methodology and the MATLAB program written for the applications of its algorithm are also included in this chapter.

Chapter 3 describes the parametric study conducted using the MATLAB program described in the previous chapter. It gives a detailed description of the parameters used in the study and the motivation behind their selection. It presents the outputs of the analyses and examines how the parameters affect the performance of the structures through statistical tools. Last but not least, it introduces the screening methodology developed using the data obtained from this study.

A summary of the study, results, and suggestions for how it may be enhanced and further explored are all included in Chapter 4.

2. ENERGY-BASED DESIGN METHODOLOGY

In this chapter, the response of structures to ground motions is discussed in terms of energy. A basic SDOF system was used as a model for the derivation of the related formulae and the energy terms. Furthermore, an Energy-Based Design algorithm which was used for the parametric study conducted for the development of the rapid screening procedure was introduced.

2.1. Energy Balance Equation

Quantifying the response of SDOF systems under dynamic ground excitations has been used by engineers to understand how more complex structures behave under seismic loads. Therefore, a basic SDOF model described in Figure 2.1 could be used to formulate this response.
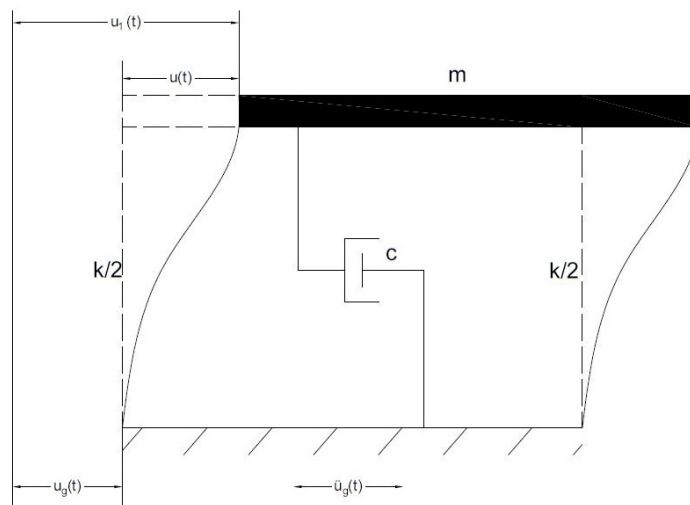
Figure 2.1. SDOF model under ground excitation.

Equation of motion of this model [6] can be summarized as

$$m\ddot{u}_t(t) + c\dot{u}(t) + f_s(u(t), \dot{u}(t)) = 0, \qquad (2.1)$$

where terms m, c, f_s correspond to the mass, damping coefficient and the spring force of

the system, respectively. The time histories of the total acceleration, relative velocity and relative displacement are, in that order, denoted by $\ddot{u}_t(t), \dot{u}(t)$ and $u(t)$. The term f_s could be defined as $ku(t)$ for linear elastic systems where k denotes the total stiffness of the system. The total acceleration response could be represented as the combination of the ground acceleration and the relative acceleration of the system as

$$\ddot{u}(t) + \ddot{u}_g(t) = \ddot{u}_t(t). \tag{2.2}$$

Therefore, Equation (2.1) can be rewritten as

$$m\ddot{u}(t) + c\dot{u}(t) + f_s(u(t), \dot{u}(t)) = -m\ddot{u}_g(t). \tag{2.3}$$

Equation (2.3) allows for the system to be remodeled as a fixed base structure with a horizontal dynamic force of $m\ddot{u}_g$.
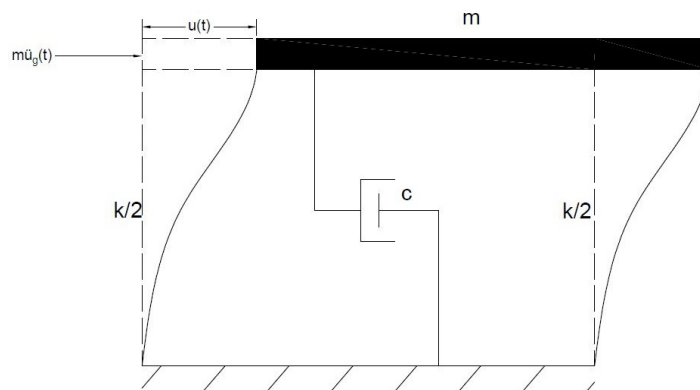
Figure 2.2. SDOF model with a fixed-base.

The main difference of the models depicted in Figures 2.1 and 2.2 is their reference points. The former expresses the response with respect to a point on the ground (absolute response) whereas the latter expresses it with respect to the initial position at rest (relative response). When Equations (2.1) and (2.3) are examined, it could be seen that only the terms related to mass differ from one another.

The equilibrium of the external and internal forces during a dynamic motion is summarized by Equation (2.3). This points out to the fact that the work done by the forces on the left hand side of the equation must be equal to the ones on the right

hand side. Akiyama [12] based the energy balance concept on the equilibrium of forces acting on a SDOF system.

2.1.1. Derivation of the Energy Formulations

Uang and Bertero [23] explained the distinction between the energy formulations based on the absolute and the relative response of SDOF systems and derived the equations in this subsection. When Equation (2.1) is integrated with respect to the displacement $u(t)$ (relative), it becomes

$$\int m\ddot{u}_t(t)du + \int c\dot{u}(t)du + \int f_s du = 0. \tag{2.4}$$

Writing the relative displacement as $u(t) = u_t(t) - u_g(t)$ and updating Equation (2.4) accordingly gives

$$\int m\ddot{u}_t(t)du_t + \int c\dot{u}(t)du + \int f_s du = \int m\ddot{u}_t(t)du_g. \tag{2.5}$$

Each term in Equation (2.5) corresponds to Absolute Kinetic Energy, Damping Energy, Absorbed Energy and Absolute Input Energy, respectively. They constitute the Absolute Energy Equation and it can be symbolized as

$$E_k + E_d + E_a = E_I. \tag{2.6}$$

Absorbed Energy term can be rewritten as the summation of Elastic Strain Energy, E_s, and Plastic Strain Energy, E_p, as

$$E_a = E_s + E_p. \tag{2.7}$$

These terms are important for the calculation of the dissipated energy of a structure under dynamic loads. If the model in Figure 2.2 (fixed-base system) is selected to be used for derivations, the end result would give the Relative Energy Equation. For this purpose, Equation (2.3) is integrated with respect to the relative displacement $u(t)$ and the modified equation is obtained as

$$\int m\ddot{u}(t)du + \int c\dot{u}(t)du + \int f_s du = -\int m\ddot{u}_g(t)du. \tag{2.8}$$

In this case, the terms in Equation (2.8), in order, correspond to Relative Kinetic Energy, Damping Energy, Absorbed Energy and Relative Input Energy and the symbolic

version of the equation can be written as

$$E'_k + E_d + E_a = E'_I. \tag{2.9}$$

Even though the energy calculated by both methods is close, the main deviation comes from the terms which include the mass of the system (Kinetic and Input Energy terms). Bertero and Uang [23] concluded that the Absolute and Relative Input energies for the structures with intermediate fundamental periods are very similar ,given the same displacement ductility. The deviation increases for the structures with very long or very short periods. This fact is important for this study as it mainly focuses on the residential structures which have intermediate periods.

2.2. Energy Terms and Their Distribution

Evaluating the terms in the energy balance equation would assist highlighting the physical characteristics of a structure since they represent various sorts of energies that develop during ground motion. Taking the derivative of Equation (2.8) with respect to time yields a more convenient equation for the calculation of these terms as

$$\int m\ddot{u}(t)\dot{u}(t)dt + \int c(\dot{u}(t))^2dt + \int f_s(t)\dot{u}dt = -\int m\ddot{u}_g(t)\dot{u}(t)dt. \tag{2.10}$$

Further simplifying Equation 2.10 gives

$$\frac{m(\dot{u}(t))^2}{2} + \int c(\dot{u}(t))^2dt + \int f_s(t)\dot{u}dt = -\int m\ddot{u}_g(t)\dot{u}(t)dt. \tag{2.11}$$

The term on the right hand side of Equation (2.11) corresponds to the input energy E_I. The first term on the left hand side of Equation (2.11) is the Kinetic Energy E_k, which represents the motion energy of the system. The second one is Damping Energy E_d, which represents the inherent energy dissipating attribute of the system. Absorbed Energy, which is the third term, consists of Elastic Strain Energy, E_s, and Plastic Strain Energy, E_p. While the Elastic Energy could be simply formulated as

$$E_s = \frac{(f_s(t))^2}{2k}, \tag{2.12}$$

Plastic Strain Energy cannot be directly calculated. Since all the other terms can be explicitly formulated as above, Plastic Strain Energy, E_p, can be expressed as the

subtraction of all the other terms from the Input Energy as

$$E_p = E_I - E_k - E_d - E_s. \tag{2.13}$$

Since the calculation of the Inelastic Strain Energy indirectly through all the other terms is inconvenient, it is traditionally preferred to obtain it by calculating the area under the force-displacement hysteresis curves of the system [24].

The energy terms examined herein fall into two main categories (see Figure 2.3), namely recoverable and irrecoverable energies [9]. The Elastic Strain Energy and the Kinetic Energy are recovered by the structure once the ground motion comes to a stop. However, Damping Energy and Inelastic Strain Energy are path-dependent and they increase with the duration of the motion.
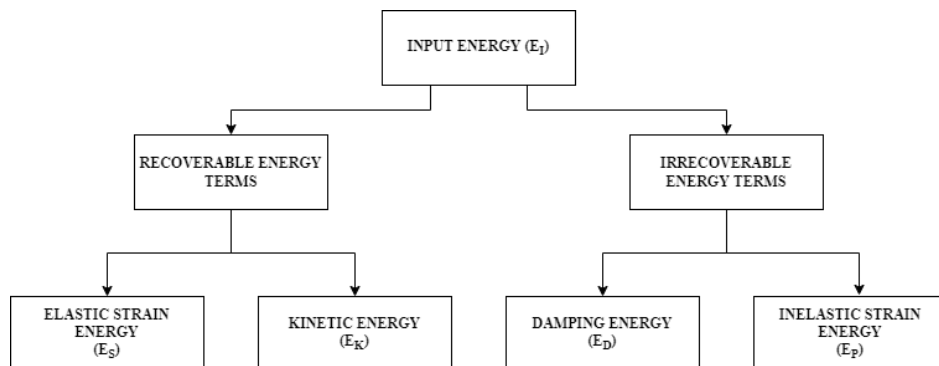
Figure 2.3. Distribution of the Energy Terms.

Understanding the dissipated energy terms is particularly significant since they are essential for calculating the damage the earthquake motion leaves on the structure [25].

2.3. Earthquake Energy Demand

Engineers have created practical techniques that aim to account for the most structural and ground motion characteristics possible due to the unpredictability of earthquakes. The seismic spectra are developed with this objective in mind. So far,

force and displacement based methods have been using these spectra to calculate the earthquake demand.

Energy demand spectra differ from the traditional elastic response spectra used in the current codes in that they take into account inelastic response as well as the duration of the earthquake and the frequency content, whereas elastic response spectra only concentrate on expected extreme values. Additionally, ductility rather than the load reduction factor is used in the energy spectra as the inelastic response parameter.

When the demand concept is examined from energy perspective, energy formulations must be taken into consideration. As was covered in the sections above, the input energy E_I, which includes all other forms of energies, is the energy that an earthquake transmits to a structure. The plastic component of the input energy E_P must be identified since it makes up the energy demand that must be compared to the energy dissipation capacity. Hence, the ratio of the plastic and hysteretic energy to the input energy must be determined and the spectra should be constructed accordingly. Several researchers worked on creating input energy spectra [16, 25–28] and developing the relationship between input and hysteretic energy [9, 13, 26]. Dindar's spectra is examined in detail in this section.

2.3.1. Dindar's Spectra

Dindar *et al.* [16] developed an algorithm for the construction of the spectra, with an SDOF model and conducted numerous nonlinear time history analyses with several parameters and ground motion records with an assumed damping ratio of 5%. Controlled parameters include 6 types of constitutive behavior models, 4 ductility levels, 4 different soil types and modal characteristics. Energy terms are calculated from the outcomes for a range of period values after this iterative process has been completed. Regression analyses are then used to produce the generalized formulations and plots of the input and plastic demand energy spectra. Figure 2.4 displays the results of the described study. The researchers concluded that the Elastic-Perfectly-

Plastic constitutive model is sufficient to account for all other models. Therefore, they used EPP model for simplicity.
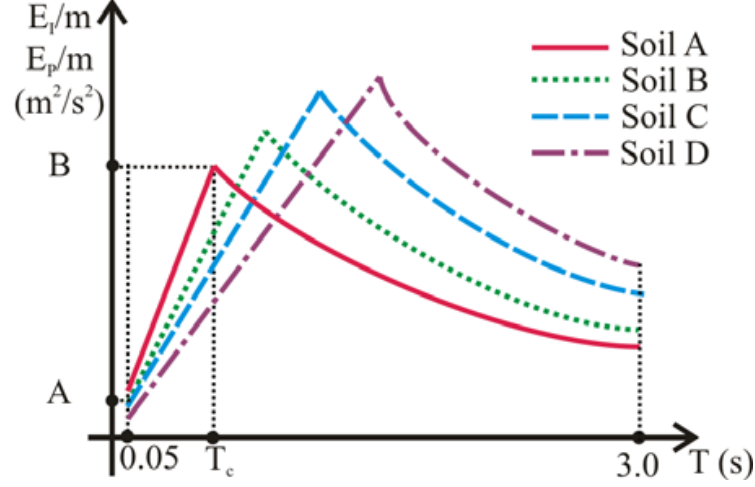
Figure 2.4. Input and Plastic energy demand spectra for different soil types with 5% damping ratio and EPP constitutive model proposed by Dindar *et al.* [16].

The Input Energy demand spectra is formulated as

$$E_I^{PGA} = (PGA/0.1g)^2 \times E_I^{0.1g} \times m. \tag{2.14}$$

PGA in Equation (2.14) is the abbreviation for Peak Ground Acceleration, m is the mass, and $E_I^{0.1g}$ is the mass normalized Input Energy for $PGA = 0.1$g. The formulation for $E_I^{0.1g}$ is

$$E_I^{0.1g} = \begin{cases} A + (B - A)(T - 0.05)/(T_C - 0.05) & 0.05s \leq T \leq T_C \\ B(T_C/T)^k & T_C \leq T \leq 3.0s. \end{cases} \tag{2.15}$$

The Plastic Energy demand spectra is formulated as

$$E_P^{PGA} = (PGA/0.1g)^2 \times E_P^{0.1g} \times m. \tag{2.16}$$

PGA in Equation (2.16) is the abbreviation for Peak Ground Acceleration, m is the mass, and $E_P^{0.1g}$ is the mass normalized Input Energy for $PGA = 0.1$g. The formulation for $E_P^{0.1g}$ is

$$E_P^{0.1g} = \begin{cases} A + (B - A)(T - 0.05)/(T_C - 0.05) & 0.05s \leq T \leq T_C \\ B(T_C/T)^k & T_C \leq T \leq 3.0s. \end{cases} \tag{2.17}$$

The parameters A, B, k and T_C are different for Input and Plastic energy formulations and can be found in Table 2.1.

Table 2.1. Parameters for Input and Plastic energy demand spectra proposed by Dindar *et al.* [16].

		Soil A		Soil B		Soil C		Soil D	
		$\mathbf{E_I}/m$	$\mathbf{E_P}/m$	$\mathbf{E_I}/m$	$\mathbf{E_P}/m$	$\mathbf{E_I}/m$	$\mathbf{E_P}/m$	$\mathbf{E_I}/m$	$\mathbf{E_P}/m$
$\mu = 1$	A (m^2/s^2)	0.0059	0.0000	0.0050	0.0000	0.0040	0.0000	0.0045	0.0000
	B (m^2/s^2)	0.0650	0.0000	0.0705	0.0000	0.0770	0.0000	0.0850	0.0000
	Tc (s)	0.5000	0.5000	0.6500	0.6500	0.9000	0.9000	1.0500	1.0500
	k	0.9100	0.0000	1.0950	0.0000	1.4560	0.0000	1.6580	0.0000
$\mu = 2$	A (m^2/s^2)	0.0051	0.0027	0.0046	0.0022	0.0038	0.0019	0.0038	0.0019
	B (m^2/s^2)	0.0551	0.0321	0.0624	0.0340	0.0650	0.0380	0.0700	0.0400
	Tc (s)	0.4500	0.4500	0.6000	0.6000	0.8000	0.8000	0.9500	0.9500
	k	0.8480	0.8280	1.0710	0.9840	1.3200	1.2700	1.5540	1.5000
$\mu = 4$	A (m^2/s^2)	0.0044	0.0030	0.0042	0.0028	0.0037	0.0024	0.0037	0.0024
	B (m^2/s^2)	0.0444	0.0306	0.0500	0.0320	0.0530	0.0350	0.0580	0.0380
	Tc (s)	0.4000	0.4000	0.5500	0.5500	0.7000	0.7000	0.8500	0.8500
	k	0.8890	0.9540	1.1070	1.1270	1.2600	1.3100	1.4500	1.5200
$\mu = 6$	A (m^2/s^2)	0.0040	0.0032	0.0035	0.0039	0.0036	0.0026	0.0036	0.0027
	B (m^2/s^2)	0.0350	0.0291	0.0410	0.0300	0.044	0.0330	0.048	0.0360
	Tc (s)	0.3500	0.3500	0.5000	0.5000	0.6500	0.6500	0.8000	0.8000
	k	0.8610	0.9500	1.1100	1.1500	1.2720	1.2800	1.4140	1.4690

2.3.2. Güllü's Spectra

Güllü *et al.* [29] proposed a modified input energy spectrum whose formulation was verified by shake table tests where a steel column is excited by a wide range of ground motion records. They also assessed the energy demand spectra existing in the literature including the spectra developed by Dindar *et al.* [16]. Their experiments

were beneficial in verifying Dindar's spectra. Most of the current spectra assume 5% damping as it is considered to be valid for concrete structures whereas in the study by Güllü *et al.* [29], steel specimens were used, which had a much lower damping ratio.

The main modification from Dindar's formulation is made by dividing the spectrum into three parts rather than two. Another critical point in the spectrum is determined by dividing the corner period T_c by 1.2. As can be seen in Figure 2.5, after the ascending branch reaches this value, the spectrum stays constant until it reaches T_c and the descending branch related to $(T_c/T)^k$ starts. The spectrum formula is

$$\frac{E_I}{m} = B\sqrt{SV(\zeta)_{max}SA(\zeta)_{@SV_{max}}T_cI_et_e}(T_c/T)^k. \tag{2.18}$$

In Equation (2.18), $SV(\zeta)_{max}$ and $SA(\zeta)_{@SV_{max}}$ correspond to the maximum spectral velocity and the spectral acceleration where the spectral velocity is maximum, all with the specified damping ration ζ. The parameters B and k used here are taken from Dindar's formulation (Table 2.1).
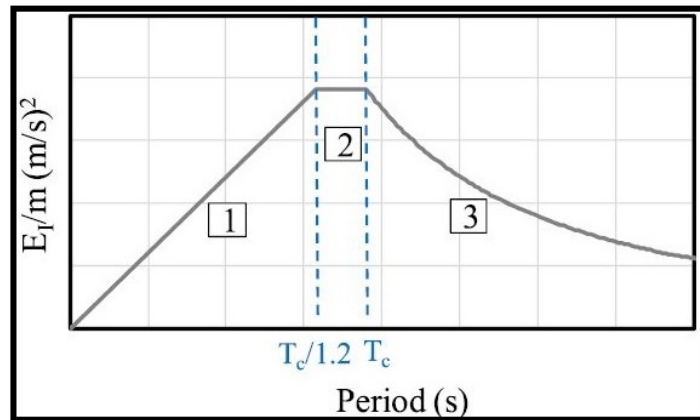
Figure 2.5. Mass-normalized input energy spectrum by Güllü *et al.* [29].

In this study, the total energy demand is calculated through the utilization of plastic energy spectra proposed by Dindar *et al.* [16] as it is also used in the methodology proposed by Yalçın *et al.* [1].

2.4. Energy Dissipation Capacity

The design approach has a significant impact on the definition of seismic capacity and the elements that determine it. Since it is the main aim of the Force-Based Design method for a structure to cope with the maximum lateral force it might take, capacity is defined by focusing on the shear capacity of beams and columns. On the other hand, Displacement-Based Design uses displacement ductility capacity and the rotation capacity of plastic hinges as the main parameters [22]. Current design methodologies ignore the damage that builds up during an earthquake's reverse cycling excitation [25]. Energy-Based Design outperforms other approaches by taking this phenomenon into account.

2.4.1. Low-cycle Fatigue Theory

Studies on low-cycle fatigue tests on RC cantilever columns linked energy dissipation to the number of cycles they experience and the degradation of strength [30]. They inferred from the experimental data that the energy dissipation capacity of columns in flexure-shear mode is very similar to the ones in only flexural mode. Another important conclusion they had is that the variable-amplitude loading could be represented from constant-amplitude loading results. These results, as stated in the paper, are only applicable for columns with an axial load ratio of less than 20%.

In [31], a series of experiments were conducted to investigate the energy dissipation characteristics of RC beams and their relation to low-cycle fatigue. They tested the specimens under constant and variable amplitude excitations. Using the experiment results, they proposed an Energy-Based low-cycle fatigue model. It was emphasized how the behavior of the members is path-dependent and memory-dependent, meaning that the cumulative energy dissipated is dependent on the number of cycles and the hysteretic path being followed. Based on the similar results of the two studies mentioned above, capacity calculations could be done through constant-amplitude low-cycle fatigue analyses to reach the total energy dissipation capacity under earthquake loading.

2.4.2. Performance Levels and Their Relation to Capacity

The capacity has been commonly associated with the drift ratios and strain levels at system level and member level, respectively [22]. With this philosophy, these parameters are used to define the performance targets in order to determine the capacity of the members or the system itself. The targets for overall structural performance and sectional performance of the members, taken from Turkish Seismic Code [32], are used for the determination of capacity in the study by Yalçın *et al.* [1]. Figure 2.6 and Figure 2.7 illustrate the targets which are also employed in this study.
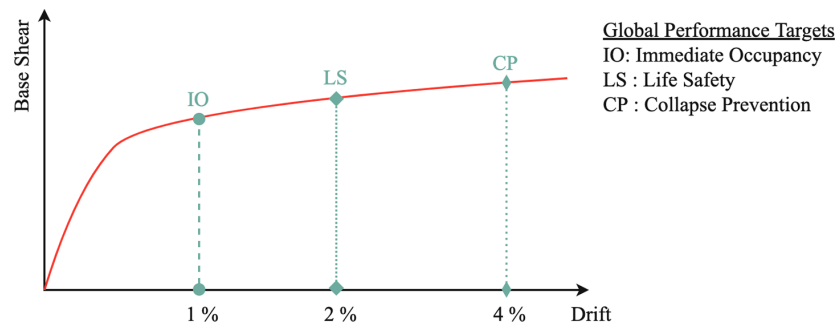
Figure 2.6. Global Performance Targets [1].
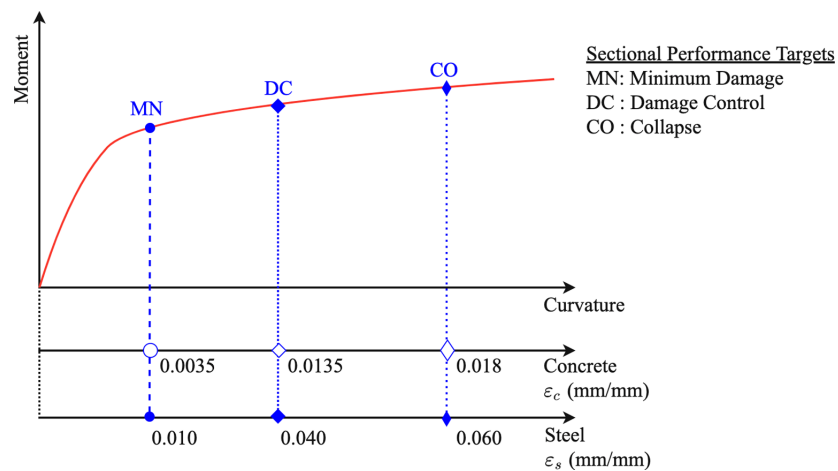
Figure 2.7. Sectional Performance Targets [1].

As can be seen in Figure 2.7, strain limits for concrete and steel are matched with curvature levels in order to determine the performance targets. For the strain levels for concrete compression and steel tension, these targets are defined at the point whichever is reached first.

2.4.3. Quantification of Damage at Member Level

The ability of a structure to sustain damage can be associated with the plastic energy dissipation capability, as researchers have shown via experimental studies [33]. The model proposed by Park and Ang [34] stands out among attempts to quantify the occurrence of damage as the one that takes the impact of energy into consideration. Park-Ang damage index formulation for reinforced concrete structures is given as

$$D_{PA} = \frac{\delta}{\delta_u} + \beta \frac{\int dEH}{F_y \delta_u}, \tag{2.19}$$

where δ is the maximum deformation during an earthquake, δ_u is the ultimate deformation from pushover analysis, F_y is the yield strength, and the terms in the integral represents the energy dissipation during the cyclic motion. D_{PA} is the damage index ranging from 0 to 1, minor to severe.

The energy-based design method proposed by Yalçın *et al.* [1] uses Park-Ang damage indices as the main damage indicator. Stop criteria for the constant amplitude low-cycle fatigue analyses are based on these indices along with 20 percent strength decrease. Damage indices corresponding to each sectional performance target are given in Table 2.2 where MN, DC and CO correspond to Minimum Damage, Damage Control and Collapse Prevention, respectively.

Table 2.2. Damage indices for section performance levels.

Performance Target	MN	DC	CO
$\mathbf{D_{PA}}$	0.2	0.4	0.6

2.5. Energy-Based Design with Performance-Based Guidelines

The Energy-Based Design methodology put forth by Yalçin *et al.* [1] is outlined in this section, along with a description of a MATLAB [35] program that implements its algorithm. This MATLAB program was specifically written to be utilized for the parametric study described in the following chapter. The methodology uses the fundamental idea behind earthquake-resistant design: a structure must be able to withstand the demand caused by ground vibrations by estimating demand and capacity using energy-based principles. The procedure for determination of input energy was developed by Dindar *et al.* [16] and the dissipated energy capacity calculations were based on Dindar's findings [9]. Through the use of performance-based guidelines, the comparison of energy demand and energy dissipation capacity is carried out.

The algorithm starts with a preliminary design of an RC frame. Demand and capacity are the next two major branches that it spreads into. The major aim of the demand branch is to model the distribution of spectral energy input values onto the structure. By using constant amplitude fatigue analyses of equivalent cantilever models, the capacity branch seeks to determine the energy dissipation capabilities of each member. On the basis of a comparison of the outcomes from these two branches, the design quality is to be evaluated. This comparison is driven by the performance criteria, either at member or structural level, established prior to the process starting. It is advised to either enlarge sections or increase reinforcement ratios if these performance requirements are not met. An iterative process goes on until the design is optimized.

It was stated by the researchers [1] that this approach is only relevant to low-to-mid rise structures which mostly exhibit first mode behavior, making it appropriate for the frame set employed in this study. Moreover, the practicality of the method allows an engineer to apply it on numerous frames to observe the effect of many parameters controlling the demand and capacity. In this sense, the MATLAB program evaluates the capacity and demand of a frame in three modules based on these parameters, namely the demand module, capacity module, and performance assessment module.

Each module in the MATLAB program contains several functions that allow the user to run the algorithm steps separately and then combine the results for final calculations.
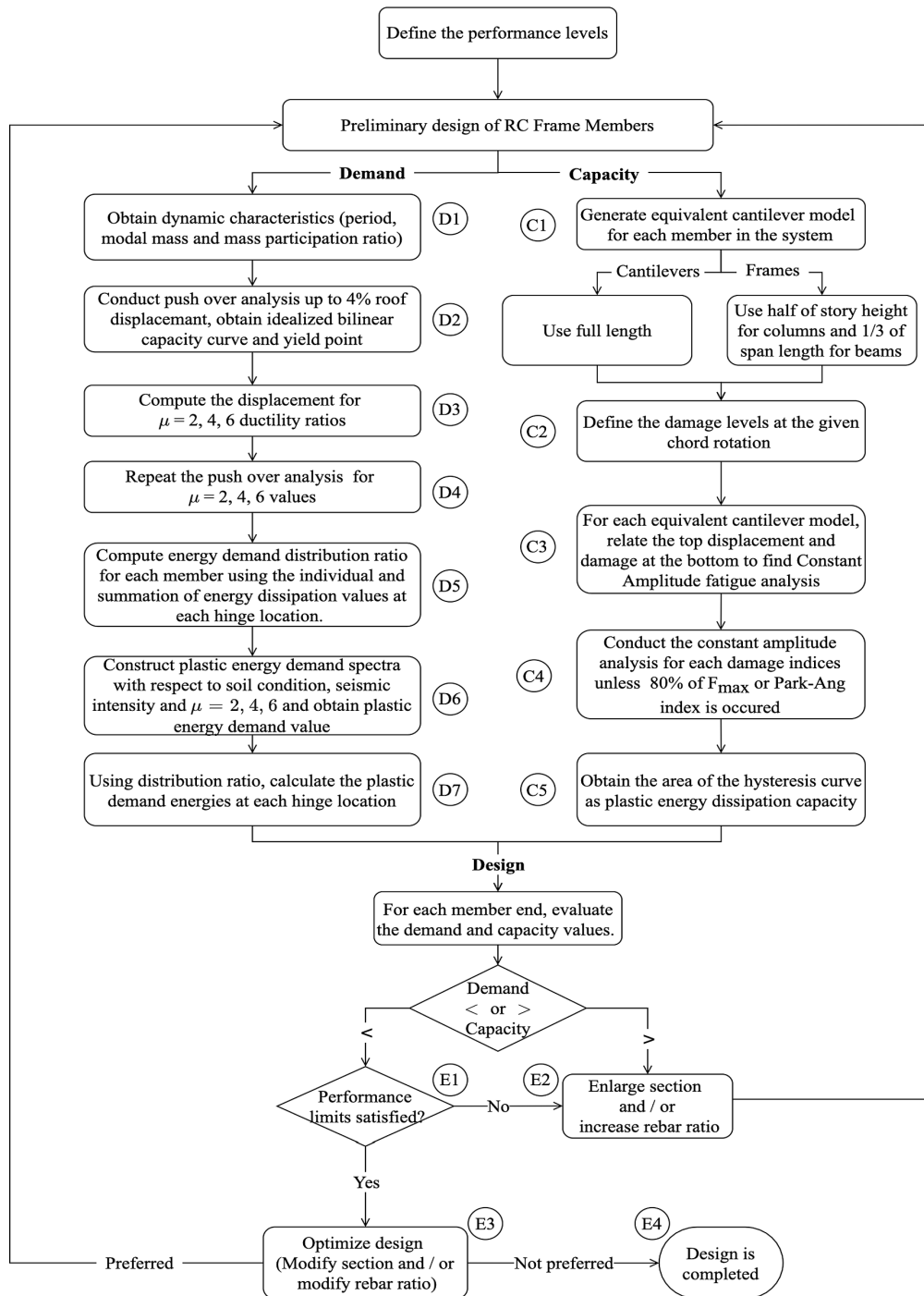
Figure 2.8. The Energy-Based Design algorithm proposed by Yalçın *et al.* [1].

2.5.1. Demand Procedure

The demand algorithm consists of the steps described below.

Since the capacity comparison is also to be done at the member level, it is also essential to calculate the distribution of the total input energy demand across the structure. Between various ductility levels, this distribution varies. Due to this, demand distribution ratios for each predetermined ductility level must be calculated.

A flowchart was developed to obtain both demand and capacity of the structures. This flowchart is given in Figure 2.8, which summarizes the algorithm described in this section. Steps C1 through C5 constitute the capacity branch whereas steps D1 through D7 are the steps for demand calculations. Steps E1 through E4 are the evaluation steps of the algorithm.

The demand branch of the algorithm starts with the acquisition of the dynamic characteristics related to the preliminary design (D1). To produce the idealize bilinear capacity curve, which provides the yield point when ductility $\mu = 1$, a pushover study up to 4 % roof displacement is then performed (D2). Following the setting of the yield displacement, roof displacements corresponding to $\mu = 2, 4, 6$ are calculated (D3). Next, three pushover analyses for these performance levels are carried out (D4).

Moment-rotation curves were generated for each hinge at each level of ductility under the assumption that each member has plastic hinges at both ends. Area enclosed by these curves yields the dissipated plastic energy. The demand energy distribution ratios are obtained by dividing the dissipated energy at each hinge location by the total energy dissipated at a certain ductility level (D5).

Plastic energy demand spectra are constructed as per Dindar's [16] formulation while taking soil type, ductility and peak ground acceleration as parameters. The spectral energy value corresponding to the structure's natural period is acquired from

the spectra. Then, it is multiplied by the total mass of the structure (D6). Finally, using the demand distribution ratios, the total plastic energy demand is distributed onto the hinges (D7). Thus, the demand branch of the algorithm is completed.

2.5.1.1. Demand Module of the MATLAB Program.   This module executes the steps associated with the algorithm's demand branch (D1-D7).

The module begins by obtaining the frame properties, which include the following:

- Concrete and steel material properties: strength under compression and tension, yield and ultimate strain values.
- Geometric properties: number of stories and their heights, number of bays and their widths.
- Column and beam section properties: section width and height, concrete cover, number and size of longitudinal rebars, size and number of lateral ties.
- Dead and live loads to be factored and distributed on the beams.
- Soil type.
- Peak Ground Acceleration (PGA)
- Presence of corrosion and bond between the reinforcement and the concrete.

The frame properties are fed into the structural analysis software SAP2000 [36]. Steps D1-D4 are carried out in the SAP2000 environment. This is made possible through the use of the API (Application Programming Interface) function of SAP2000. API allows the user to define structures in detail, conduct several types of analyses and acquire the results from an external software such as MATLAB, Visual Basic, Python etc. Benefiting from this property, a MATLAB function which uses API is written and used within the demand module. From the properties itemized above, the function creates a model in SAP2000 using a simple frame matrix and assigns sections to each member of the frame. It applies the factored distributed loads onto the frame based on the load combination for nonlinear static pushover analysis stated in 2018 Turkish Seismic Code [22]. The load combination takes the dead load as it is and multiplies

the live load by 0.3. Lumped plasticity model is used and the effective flexural stiffness $(EI)_e$ values for beams and columns are calculated using TSC's [22] equation

$$(EI)_e = \frac{M_y}{\theta_y} \frac{L_s}{3},$$ (2.20)

where M_y, θ_y, and L_s are effective yield moment, yield rotation and shear span, respectively. As a final step of creating the frame model, plastic hinges are assigned at both ends of the members. This is one of the only two steps in this module, which requires a manual intervention as SAP2000 API does not have a function for assigning plastic hinges. Figure 2.9 is a snapshot showing the hinges assigned on the frame. SAP2000 incorporates the ASCE 41 [37] hinge properties. On this basis, it becomes easy to assign to the RC elements a predefined hinge specified for the evaluation of the existing buildings.
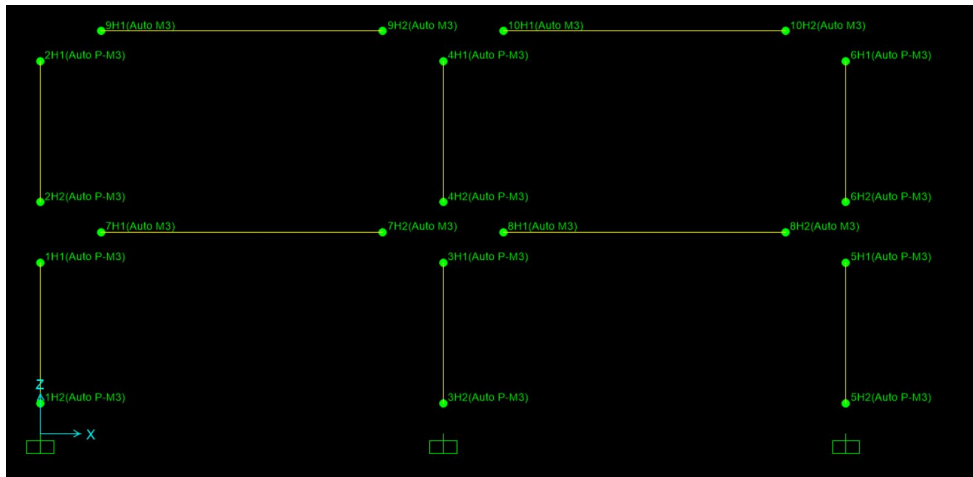
Figure 2.9. Example Frame with Hinges.

Once the frame model is complete, a modal analysis is performed to obtain dynamic characteristics such as periods, modal masses, and mass participation ratios (D1). It checks if the contribution of the first mode is greater than 70%, as this is an assumption of the method.

A nonlinear static pushover analysis is conducted where the tip displacement is selected to be 4% of the total height. SAP2000 generates a capacity curve with base

shear on the y-axis and tip displacement on the x-axis as an output of this analysis. A MATLAB function is written for the purpose of bilinearizing the capacity curve based on the equal energy principle. This principle suggests that the yield point should be determined so that the area under the bilinearized and the original curve are equal [38]. This way, the yield point is found (D2).
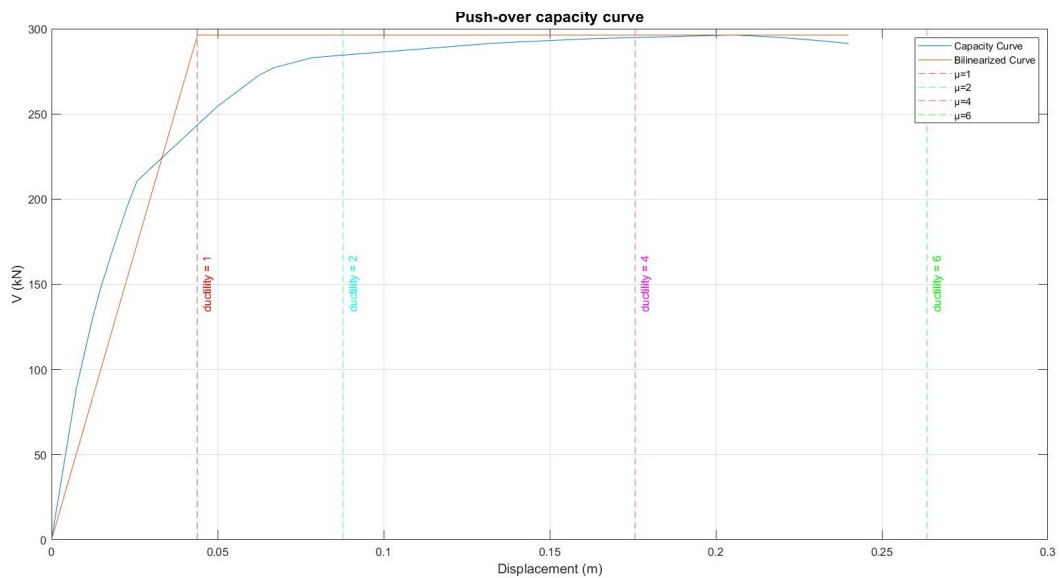
Figure 2.10. Original and Bilinearized Capacity Curves.

Figure 2.10 shows the original and bilinearized capacity curves. Using the yield point found in the previous step, displacements corresponding to $\mu = 2, 4, 6$ are calculated and marked on the plot (D3). In step (D4), three more pushover analyses are conducted for roof displacements found in the previous step.

SAP2000 generates tables for the state of hinges at each step of the pushover analysis. The moment and plastic rotation data for each hinge are listed in these tables at each stage. The second instance where manual intervention is required by the program is here since the tables cannot be exported automatically. Importing hinge moment-plastic rotation curves into MATLAB allows for the calculation of the area enclosed by the curves, which correspond to the plastic energy that has been dissipated during each analysis. Hence, individual dissipated energy values for each hinge at each

analysis are calculated and they are divided by the summation to construct the energy demand distribution ratio table (D5).

Dindar's spectra are used in this method, as was already mentioned, to determine the total input and plastic energy applied to the structure. To generate these spectra, a MATLAB function was written. This function accepts the following variables as inputs: soil type, PGA, mass, ductility, and first mode period. While the first two are predetermined before the algorithm even begins, the last three are obtained from the results of SAP2000 analyses. The MATLAB function plots plastic and input energy demand spectra based on the factors in Table 2.1. The function calculates the mass normalized energy values as a function of period and marks the point where the frame's first mode period is located. Obtained values are then multiplied by the frame's total mass. This process is repeated for $\mu = 1, 2, 4, 6$ (D6).
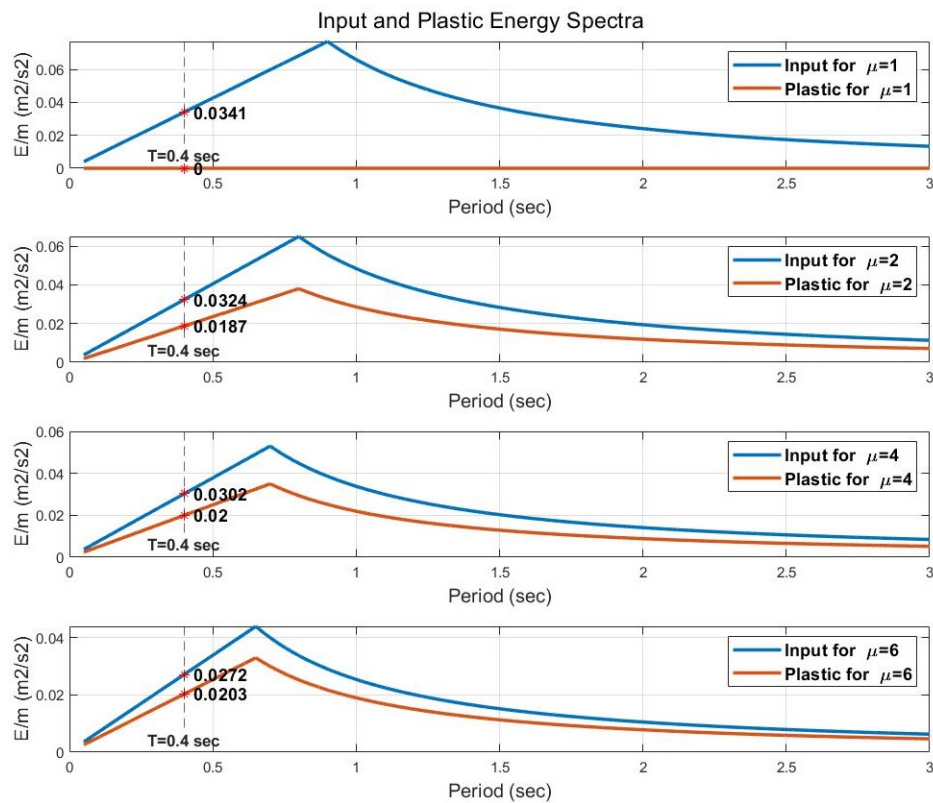
Figure 2.11. An example output of the demand spectra function.

Figure 2.11 shows an example output of the spectra function with parameters : mass= 50 metric tons, PGA=0.4 g, period= 0.4 s, soil type= C.

In order to determine the energy demand for each hinge location for various ductility ratios, the distribution ratio matrix is multiplied with the total plastic energy demand value obtained in (D6) as the last step of the demand module (D7). Hence, the demand module is concluded and the module has output these values to be compared with the capacity module results during the performance assessment procedure.

2.5.2. Capacity Procedure

The capacity algorithm consists of the steps described below.

As a first step, equivalent cantilever models are created using the presumption that, when subjected to lateral forces, the inflection points for columns are roughly in the middle and for beams, at one third of the span. Another assumption made here by the researchers is that axial loads and shear forces could be represented by the flexural behavior of the cantilever columns [1]. Therefore, representative SDOF systems are created for each member (C1).

Moment-curvature analyses conducted for all sections and performance targets given in Figure 2.7 (C2) are matched with the chord rotations based on the result of these analyses. Next, pushover analyses are carried out in order to obtain the constant amplitude corresponding to each damage level by matching the rotations with tip displacement (C3).

Quasi-static cyclic analyses with constant amplitudes obtained in preceding steps are conducted until the damage indices given in Table 2.2 are reached or 20% of the strength is lost (C4).

Finally, from the results of the cyclic analyses, the energy dissipation capacity of members at each performance target is acquired by calculating the area enclosed by the moment-rotation curves (C5). Dindar [9] inferred from his study that the energy dissipation capacity increases with increase in stiffness, reinforcement ratio, and concrete compressive strength whereas it decreases with increase in axial load level. As the shear span gets bigger, the capacity might increase or decrease depending on axial load level, reinforcement ratio, and performance targets.

2.5.2.1. Capacity Module of the MATLAB Program.   This module executes the steps associated with the algorithm's capacity branch (C1-C5).

In addition to being carried out in MATLAB environment, the analyses in this module are primarily performed using the inelastic damage analysis program IDARC2D [39], created by researchers at The State University of New York, Buffalo. The program was developed for conducting nonlinear static or dynamic analyses which are backed up by experimental study results. The fact that a fatigue-based damage model is incorporated into the program makes it perfect for understanding capacity under cyclic earthquake motion. The damage model is applicable both for nonlinear pushover and quasi-static cyclic analyses.

Modeling the hysteretic properties of the cantilever columns in this study is crucial as they dictate the behavior under cyclic loads. IDARC2D has two main hysteretic models, namely the polygonal and smooth hysteretic models. Both models have several control parameters defining the behavior, including but not limited to stiffness degradation (α), strength degradation (β_1, β_2), slip (R_s, σ, λ), and unloading shape (η). Figure 2.12 shows how stiffness and strength degradation affect the formation of hysteresis curves [39].

(a) Stiffness Degradation. (b) Strength Degradation.
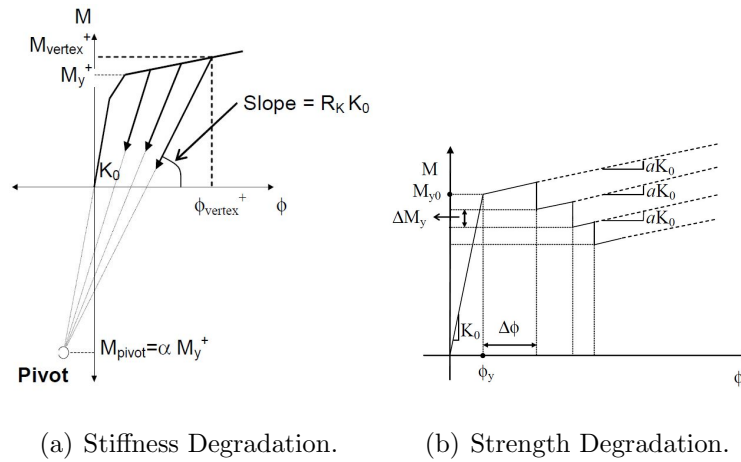
Figure 2.12. Stiffness and Strength Degradation Models.

Surmeli [40] modeled and experimentally verified the behavior of precast concrete columns under cyclic loadings using IDARC2D. By comparing the experimental and numerical results, he determined the most suitable set of control parameters after modeling the behavior using a tri-linear smooth hysteretic model. Figure 2.13 displays his success in simulating the behavior of RC columns. Dindar [9] used the mean of the values found and calibrated by Surmeli [40]. These parameters, which were also used in this study, are given in Table 2.3.

Table 2.3. Smooth Hysteresis Model Control Parameters.

α	β_1	β_2	R_s	σ	λ	N	η
3	0.10	0.10	0.09	0.03	0.60	2	0.49

In contrast to demand module, which analyzes the entire frame and looks at the distribution of energy, the capacity module evaluates each member individually first before drawing conclusions about the entire frame. Therefore, the equivalent cantilever models for column and beams are generated in the first step (C1) that will be individually examined. This is accomplished by the module by importing the mechanical properties of the beam and column sections, then dividing the span length by 2 for columns and 3 for beams.
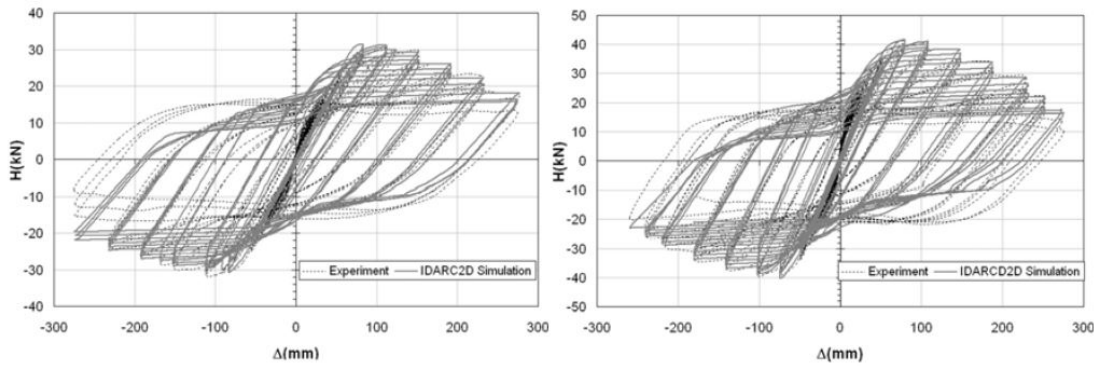
Figure 2.13. Hysteresis curves comparison of experiment results and IDARC2D

models [40].

Step (C2) requires for the curvatures corresponding to each of the performance targets given in Figure 2.7 to be calculated through sectional analyses. Moreover, sectional properties are required by IDARC2D when defining the sections for pushover and cyclic analyses making it necessary for them to be fed into the MATLAB program from a previously prepared file. A tri-linear moment-curvature relationship given in Figure 2.14 is adopted by IDARC2D for modeling the section based on its behavior. In addition to the traditional bilinear moment-curvature curves, the cracking point is introduced here, M_{cr}, and the related curvature is calculated through the initial flexural rigidity. The parameter EI3P is defined as the percentage ratio of slope after the yielding point to the slope at the origin.

P-M interaction diagrams are also necessary to model the sections to account for the effect of normal axial load. IDARC2D has its own notation when defining P-M interaction curves. This relation is given in Figure 2.15. The solid line represents the IDARC2D envelope whereas the dashed line reflects the P-M analysis results. Both of the diagrams mentioned here are construced for each section which are verified by the sectional analysis software XTRACT [41].
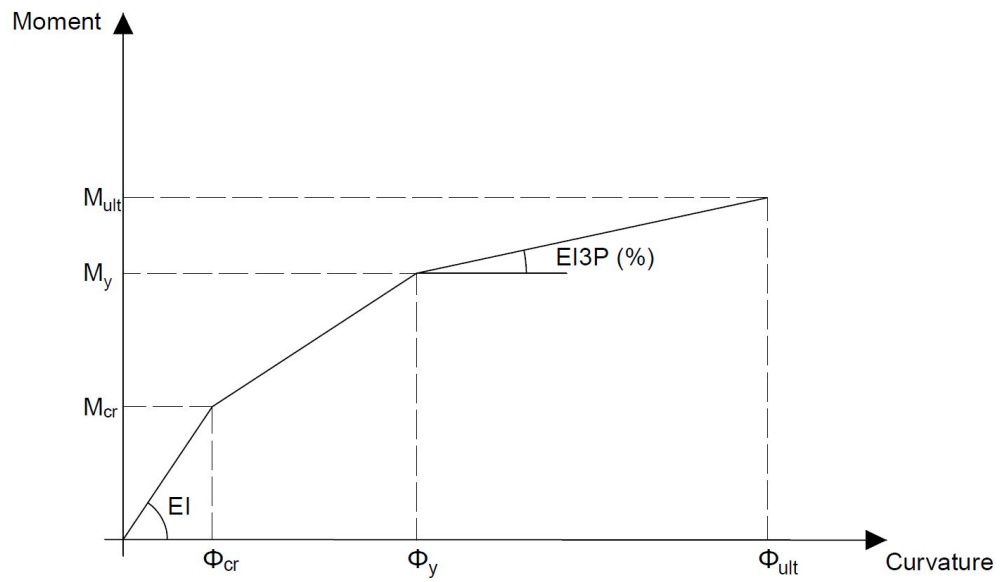
Figure 2.14. Idealized Trilinear M-K Relationship.
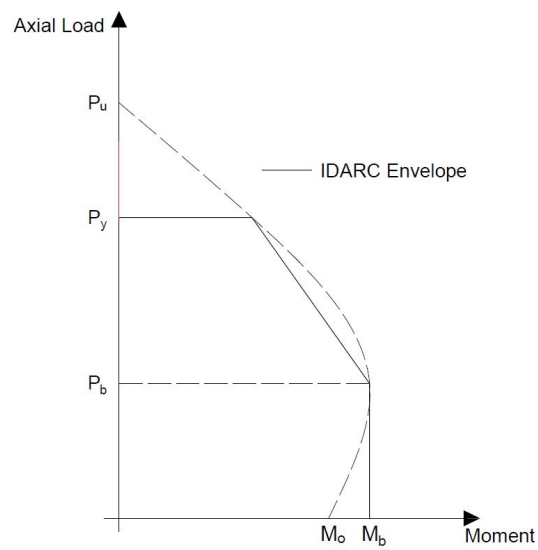
Figure 2.15. P-M Interaction Diagram.

Once all parameters in the diagrams are imported into the module, a nonlinear pushover analysis is conducted for each section. The analysis is conducted by creating an IDARC2D file and inputting sectional properties and analysis parameters. Once the analysis is complete, the tip displacements corresponding to each of the performance

targets, which are defined by the curvatures found in step (C2), are determined (C3). An example output of the pushover analysis is given in Figure 2.16.
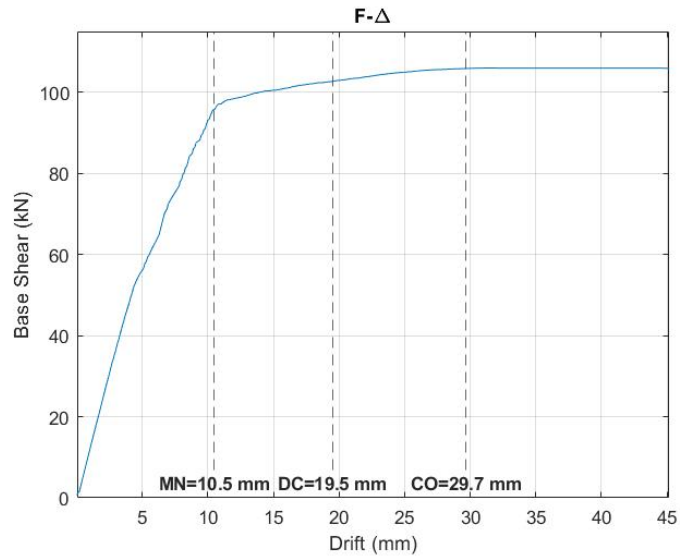
Figure 2.16. Example Pushover Curve and Tip Displacements.

Three constant amplitude fatigue analyses are conducted with three tip displacements found in (C3). The cyclic analyses are carried on by increasing the number of cycles in each iteration until the damage indices given in Table 2.2 are reached or the strength is reduced by 20%. IDARC2D output file includes the damage indices at each step of the analysis along with the force-displacement values. Therefore, the MATLAB code checks if the damage levels are reached after each iteration and also checks the strength (C4). Hence, three load-deformation hysteresis curves are produced by the program. For each performance target, the area enclosed by these curves, which is the plastic energy dissipation capacity, are calculated (C5). An example output of the module is given in Figure 2.17. This type of output is produced for each section.

Thus, the capacity module is completed and the module outputs these values to be compared with the demand module results in the performance assessment procedure.
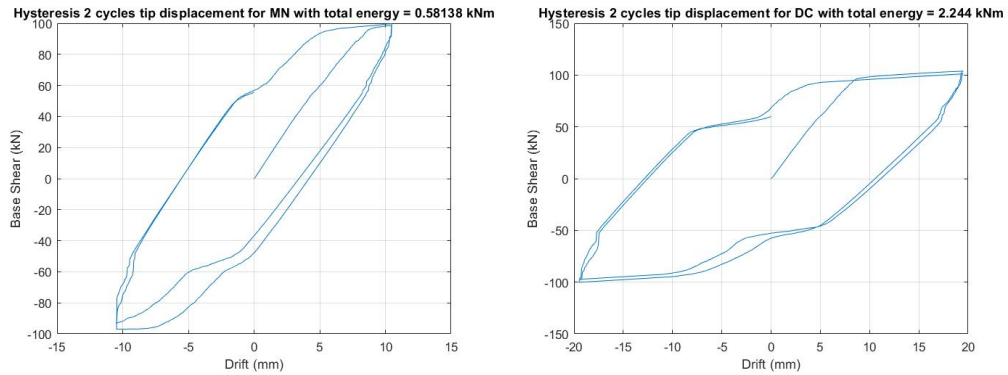
(a) Hysteresis for MN.

(b) Hysteresis for DC.
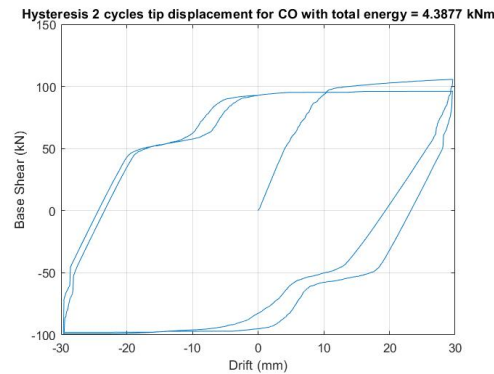
(c) Hysteresis for CO.

Figure 2.17. Example Output of the Capacity Module.

2.5.3. Performance Assessment Procedure

Once both branches of the algorithm are completed, the demand and capacity values are compared for each member and the energy-based performances at each ductility level are determined. Necessary revisions, might be increasing the size or reinforcement ratio of the members or modifying material properties, are done based on the results and the algorithm is repeated in an iterative manner.

Since it is the aim of this study to assess existing structures, a final overall performance for the structure must be determined. For this purpose, a performance assessment module has been added to the MATLAB program. The output of this module is crucial for the parametric study explained in the next chapter.

2.5.3.1. Performance Assessment Module of the MATLAB Program. This module assesses the outputs of the two preceding modules. The module retrieves the matrices containing the energy values for each ductility level and sectional performance level from demand and capacity modules, respectively. While keeping the ductility level constant, it evaluates each hinge on the frame and assigns a performance level. Finally, it plots the frame and hinges with each hinge color coded with their respective performance levels.

Figure 2.18 shows example outputs for a 2-bay 2-story frame at three ductility levels, 2,4 and 6. The colors blue, green, yellow and red represent the minimum damage (MN), damage control (DC), collapse prevention (CP), and collapse (CO) sectional performance levels, respectively.

(a) Performance at $\mu = 2$ (b) Performance at $\mu = 4$
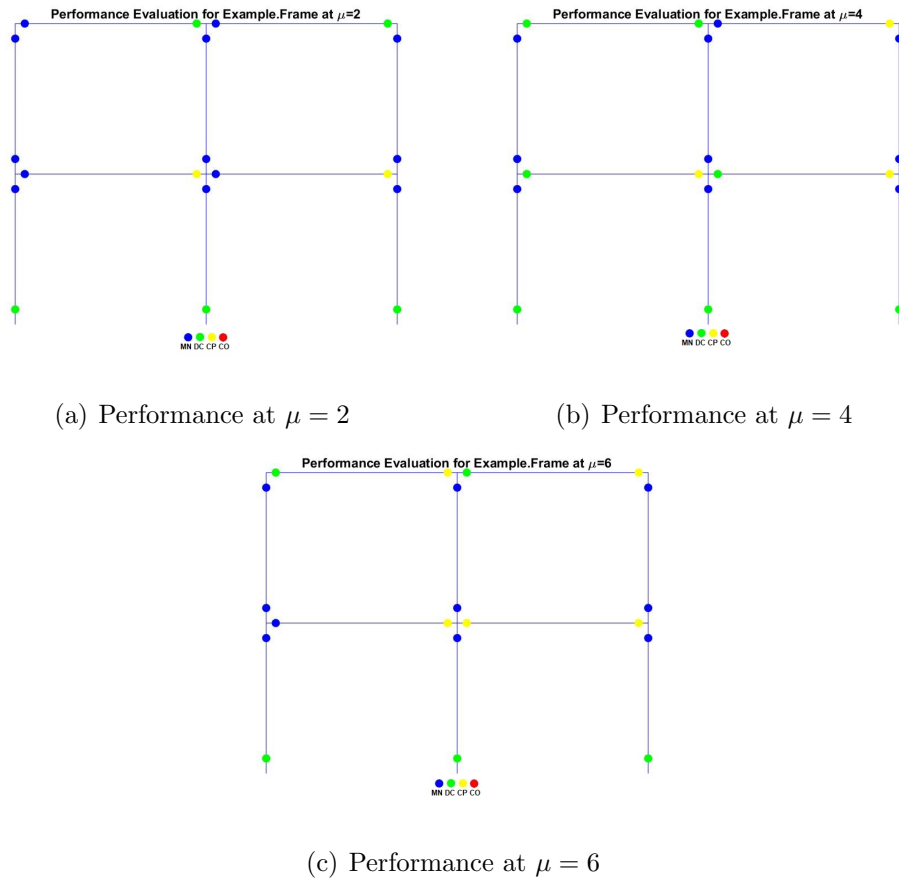
(c) Performance at $\mu = 6$

Figure 2.18. Example Output of the Performance Assessment Module.

The material and geometrical properties of the model in the figures were taken from the benchmark frame used in [1]. These results verify the accuracy of this program as the sectional performance levels of the members match the ones found in the study.

While each member's performance is known at the last step, the frame's overall performance has not been established yet. Although there are several methods for the determination of the overall performance in the literature [32, 42, 43], the guidelines in TSC 2018 [22] are used in this module as it is written for the evaluation of the buildings in Turkey.

There are four main performance levels defined in TSC 2018 section 15.8 (Determination of the Performance Levels of the Existing Buildings) for the existing RC buildings: Limited Damage, Controlled Damage, Collapse Prevention, and Collapse. Respective guidelines are given below:

- Limited Damage Performance Level Requirements: For each possible earthquake direction, maximum 20% of the beams on any floor may exceed the minimum damage level. All other load bearing elements should be at minimum damage level.

- Controlled Damage Performance Level Requirements: For each earthquake direction, maximum 35% of the beams on any floor, with the exclusion of secondary beams, may exceed the damage control level. The columns which exceed the damage control level are not allowed to carry more than 20% of the total shear force carried by all of the vertical elements on their floor with the exception of the ones on the roof level which may carry up to 40%. All other load bearing elements should be either at minimum damage level or damage control level. However, the columns which exceed the damage control level at both ends are not allowed to carry more than 30% of the total shear force carried by all of the vertical elements on their floor.

- Collapse Prevention Performance Level Requirements: For each earthquake direction, maximum 20% of the beams on any floor, with the exclusion of secondary

beams, may exceed the collapse prevention level. All other load bearing elements should be either at minimum damage level, damage control level or collapse prevention level. However, the columns which exceed the damage control level at both ends are not allowed to carry more than 30% of the total shear force carried by all of the vertical elements on their floor.

- Collapse Performance Level: Any structure unable to meet the requirements of the Controlled Damage Performance Level, it is considered to be at Collapse level.

The guidelines listed above are employed into the Performance Assessment Module and the overall structural performance level is generated.

Figure 2.19 shows the detailed flowchart of the MATLAB program described in this section. While the majority of the program is run in the MATLAB environment, the flowchart shows that the demand and capacity modules, respectively, employ external programs SAP2000 and IDARC2D. The statistical studies for the development of the screening method utilize the program's results.

The primary distinction between this flowchart and the algorithm previously mentioned is that this flowchart is intended to evaluate an existing structure rather than to design a new one.
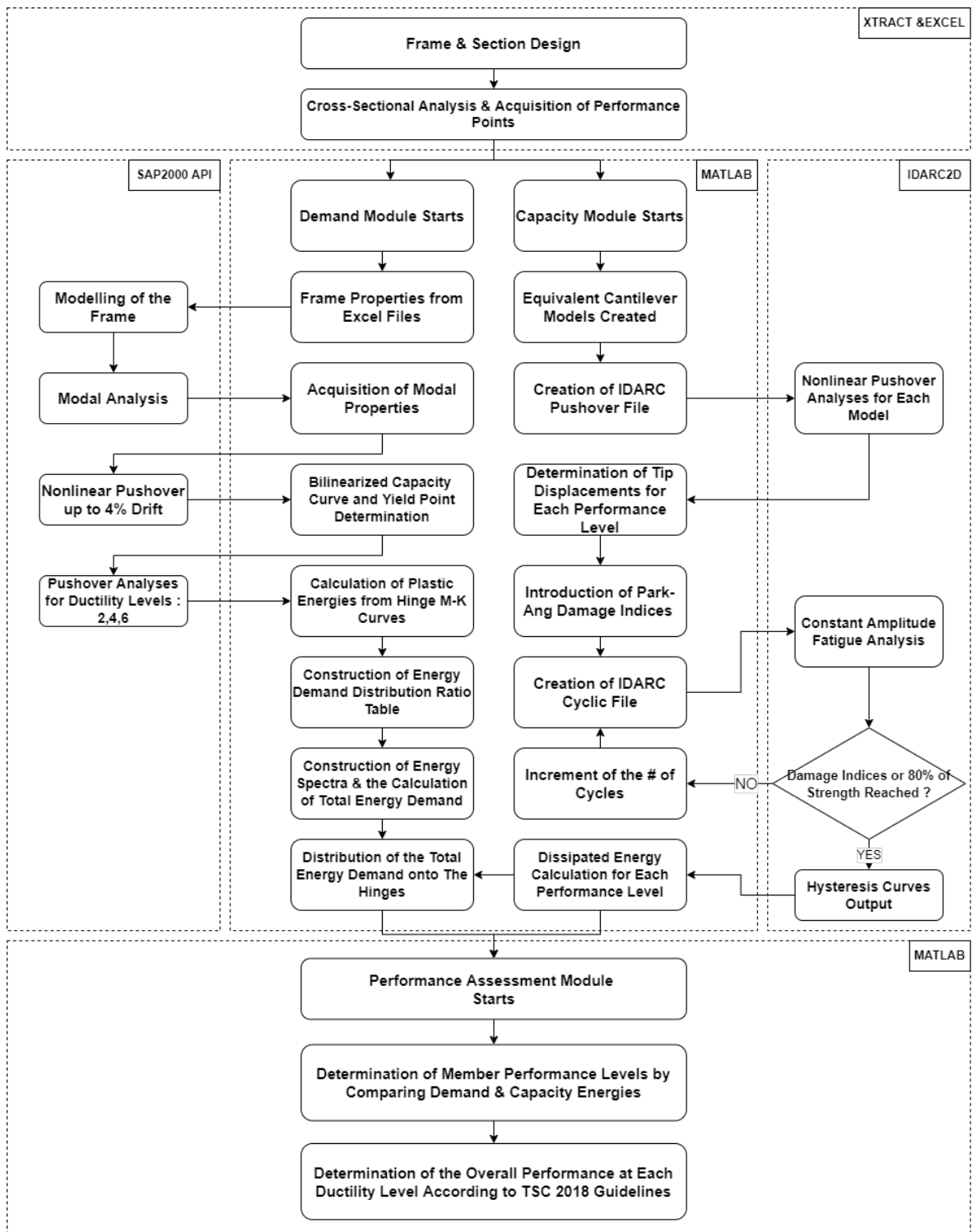
Figure 2.19. Detailed Flowchart of the MATLAB program

3. THE PARAMETRIC STUDY AND THE DEVELOPMENT OF THE SCREENING METHOD

This chapter explains the parametric study conducted for the development of the rapid screening method in detail. The analyses for the parametric study were carried out using the MATLAB program explained in the preceding chapter. The screening method's foundation was the data set that the program's output provided. This way, energy-based and performance-based principles were incorporated into the method. The data set was subjected to statistical analyses in order to determine the impact of each parameter on performance.

3.1. Building Models and Parameters

The building models and parameters used in this study were chosen to reflect the most prevalent characteristics of residential buildings in Turkey. While some of the parameters focus on the geometry, seismic zone or the geological properties, others are intended to reflect the irregularities and deficiencies may be found in residential buildings. It is noteworthy to mention that the list of parameters here is not exhaustive and the building models do not cover every possible structure. Only the ones in the scope of this study and conforming to the limitations of the energy-based methodology were included.

3.1.1. Frame Geometry and Loads

In this study, moment resisting reinforced concrete frame models which only consist of beams and columns were used. Shear walls were not included as most of the existing structurally deficient structures do not have load bearing walls. Also the effect of infill walls was excluded.

The methodology used in this study is only applicable to low to mid-rise structures which encompass most of the residential structures. A set of frames with 3 to 9 stories were created using this concept. These frames have 4 bays which are 6 meters in length. Story height was taken as 3 meters, except for soft stories, which were 4 meters in height. Number of bays and stories were included in the analyses as discrete variables.

Preliminary analysis results have shown that the number of bays has no significant impact on the performance of a structure. Therefore, in this study, this parameter was fixed. Details of how this conclusion was reached could be found in the Statistical Analysis section of this chapter. Distributed dead (G) and live(Q) loads were taken as 20 kN/m and 7.5 kN/m, respectively. These loads were factored using the load combination $w = G + nQ$, where the factor n was taken as 0.3. The influence of axial load on energy dissipation capacity of columns was proven by Dindar [9] to be of great importance. Therefore, the sections were designed in line with the axial loads they carry. Moment-curvature relationships were constructed accordingly.

3.1.2. Section Design

Sections with several deficiencies were designed along with TSC compliant ones for comparison. The most common deficiencies were chosen as: lack of adequate concrete compressive strength, lack of adequate reinforcement ratio, and lack of confinement. Column dimensions were selected to have 500 mm depth and 500 mm width whereas beam dimensions were selected to have 500 mm depth and 300 mm width. All sections were assumed to have a concrete cover of 25 mm. Longitudinal reinforcement diameters were selected to be between 14-20 mm depending on reinforcement ratio. Transverse reinforcement (if present) diameter was selected to be 8 mm. Tie spacing is 100 mm for confined sections. This value is often found to be around 200-300 mm for existing buildings, which causes a significant decrease in performance, as this study also shows with the sections with inadequate confinement.

3.1.2.1. Concrete Compressive Strength. Poor concrete quality is a common deficiency among Turkish residential buildings. This is primarily a result of improper applications and inferior production techniques. Concrete's compressive strength f_{ck} was used as a continuous parameter to simulate this deficiency, and cases with values between 8 MPa and 20 MPa were examined.

3.1.2.2. Reinforcement Ratio. Longitudinal reinforcement ratio, ρ, was used as another parameter in this study. Ranging from 0.7% to 2%, it was taken as a continuous parameter. The reason why a ratio below 1% is used is that this parameter could be frequently seen to drop under 1%. In some instances, even when the ratio is suitable, reinforcement cannot function properly with concrete due to corrosion and a lack of bonding. As a result, a low value, like 0.7%, was required.

3.1.2.3. Confinement. Numerous studies have demonstrated that confinement of RC sections has a significant impact on the behavior [44–46]. This important property is often overlooked and poor detailing provided in residential structures. Hence, the presence of confinement was included in the analyses as a parameter. Confined and unconfined material models proposed by Mander [46] were used both for moment-curvature calculations and SAP2000 analyses. Confined sections are properly detailed according to TSC [22] whereas the rest was assumed to have no confinement. Even though there is a significant reduction in performance when there is no confinement, having two extremities in the parametric study allows the inclusion of engineering judgment in the screening process due to the many levels of confinement in existing structures. Confinement was included in the data set as a binary variable (0=No Confinement, 1=Sections have adequate confinement).

3.1.3. Presence of Soft Story

The term "soft story" describes an irregularity where one floor has significantly less lateral stiffness than the others. This frequently happens as a result of the height

difference. It is known to increase the drift demand of the structure in addition to the energy accumulation on the soft story. The difference in behavior when the bottom floor is higher than the other floors is shown in Figure 3.1.
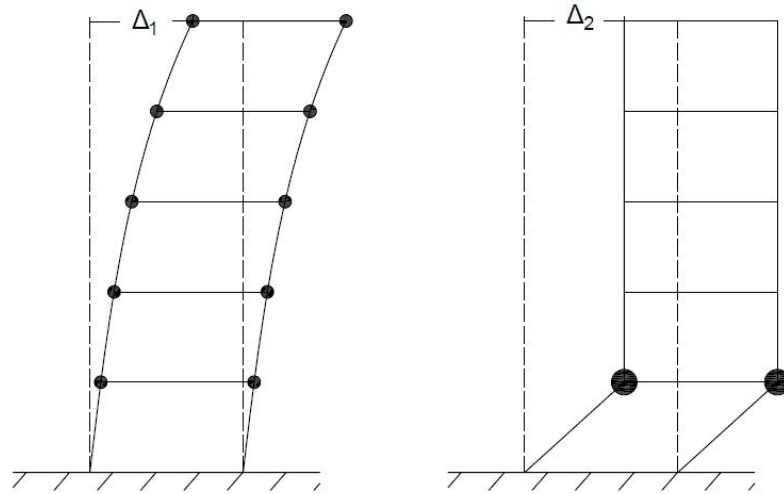
Figure 3.1. Soft Story Behavior

Case study done by Yalçın *et al.* [1] displays the occurrence of improper distribution of the energy demand when the soft story phenomenon is present in the structure. While the benchmark frame they examined is only 2 stories, it is safe to suggest that the uneven distribution of energy would get worse as the number of stories increases. The common occurrence of soft story in Turkish residential structures, mostly for commercial purposes, is one of the driving forces behind the investigation into how its presence affects performance analysis.

Soft story was included in the data set as a binary variable (0=Structure does not have any soft story, 1=Structure has a soft story).

3.1.4. Soil Type, PGA & Ductility

Soil type, PGA, and ductility are three of the key parameters used in this study's energy-based methodology to determine earthquake energy demand. A building model

must be examined in various scenarios where these parameters are different because a given structure may exist in several different places.

Four different soil types—A, B, C, and D—were included in the Dindar's spectra used in this study. In the analyses, where letters A, B, C, and D are matched with numbers 1, 2, 3, and 4, respectively, the soil type was treated as a categorical variable.

Turkish Seismic Hazard Map, published by AFAD in 2018 [47], was examined for the selection of PGA values. The PGA of the earthquakes, which have a 10% chance of occurring in 50 years, are displayed on the map. A good range for the structures in Turkey appears to be between $0.1g$ and $0.5g$. Therefore, 5 different PGA values —0.1, 0.2, 0.3, 0.4, and 0.5— were included in the analyses. In order to allow for the use of intermediate values, PGA was treated as a continuous variable.

Three ductility levels —2, 4, 6— were used in the analyses but ductility was taken as a continuous parameter for the aim of extracting information about intermediate values so that the engineer using the rapid screening method can have the option of working with different target ductility levels.

3.2. Analyses & Outputs

The parameters used in this study, as described in the previous section, are summarized in Table 3.1. Examining all combinations of these three parameters required 60 different assessments on a particular building model. This significantly expanded the number of data used in the statistical analyses and broadened the method's potential applications.

144 building models were generated and each one was examined for 60 scenarios, producing a total of 8640 data points. Building models were named based on the parameters of the study. An example name would be : $5\_4\_20\_1\_NC\_ss$ where the first four numbers represent the number of stories, number of bays, concrete compressive

strength, and reinforcement ratio, respectively. "No Confinement" and "Soft Story," respectively, are denoted by the abbreviations NC and ss.

Table 3.1. Parameters used in the study.

Parameters	Values
# of Stories	3-9
# of Bays	4
f_{ck} (MPa)	8-20
ρ_l (%)	0.7-2
Confinement	0, 1
Presence of Soft Story	0, 1
Soil Type	1, 2, 3, 4
PGA (g)	0.1-0.5
Ductility	2, 4, 6

Once all the analyses are complete, a data table was created. In this table, the rows represented the cases whereas the columns represented the building parameters, soil type, PGA, and ductility. One last column containing the performance level obtained from each case was added. The performance levels were denoted with numbers ranging from 0 to 1 where Limited Damage, Controlled Damage, Collapse Prevention, and Collapse leves are matched with 0.25, 0.50, 0.75, and 1.

A portion of the data is given in Table 3.2. Terms "n_s","n_b","C","SS" in this table correspond to number of stories, number of bays, confinement, and soft story, respectively. A more detailed table of the outputs is given in Appendix A.

Although studying the parameters one by one is insufficient to describe the entire data set, trendlines for each parameter were produced from scatter plots to better understand how each parameter influences performance. Figures 3.2 through 3.8 show the performance as a function of the parameters used in this study. Plots of each

parameter were generated for each soil type and combined in a single graph.

Table 3.2. Example outputs of the parametric study.

Frame Name	n_s	n_b	f_{ck}	ρ	C	SS	μ	PGA	Soil	Perf.
3_4_14_0.7_C	3	4	14	0.7	1	0	2	0.3	1	"CD"
3_4_14_0.7_C_ss	3	4	14	0.7	1	1	2	0.3	1	"CD"
3_4_14_0.7_NC	3	4	14	0.7	0	0	4	0.3	3	"CO"
5_4_20_1_C	5	4	20	1	1	0	2	0.4	3	"CP"
5_4_20_1_NC	5	4	20	1	0	0	6	0.5	2	"CO"
5_4_20_2_C	5	4	20	2	1	0	2	0.1	4	"LD"
7_4_20_0.7_C	7	4	20	0.7	1	0	4	0.2	4	"CD"
7_4_14_2_NC	7	4	14	2	0	0	2	0.3	2	"CO"
7_4_20_0.7_NC_ss	7	4	20	0.7	0	1	6	0.3	1	"CO"
9_4_8_2_C	9	4	8	2	1	0	2	0.4	2	"CD"
9_4_20_2_C	9	4	20	2	1	0	6	0.5	4	"CP"
9_4_8_2_C_ss	9	4	8	2	1	1	4	0.5	2	"CP"

The orange and blue dots (stacked on top of each other due to the discreteness of the data) in the scatter graphs denote the data points obtained from the analyses whereas the curves are the lines fitted to demonstrate the change in the data. It is critical to note that the y-axis in all graphs indicates the performance spectrum, with 0 representing no damage and 1 representing collapse level.

All graphs show that as the soil type changes from A to D, the performance of a structure degrades. This is due to the increase in earthquake energy demand. Figure 2.4 depicts the shift in spectra with respect to soil type, with which these findings correlate.

Figure 3.2 suggests that damage levels decrease as f_{ck} rises, as one might expect. However, this reduction does not appear to be significant. It could be deduced that

improving concrete quality may not be sufficient to improve a structure's performance when there are other flaws in the structure.
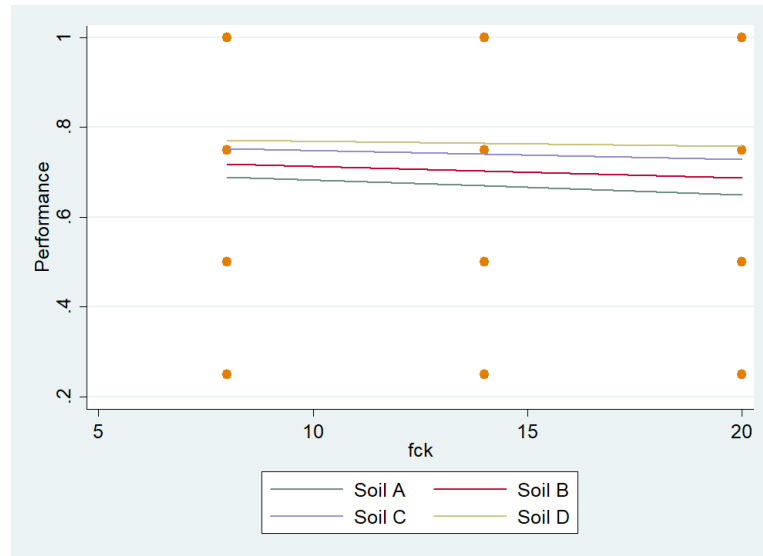
Figure 3.2. Scatter plot of f_{ck} vs. Performance
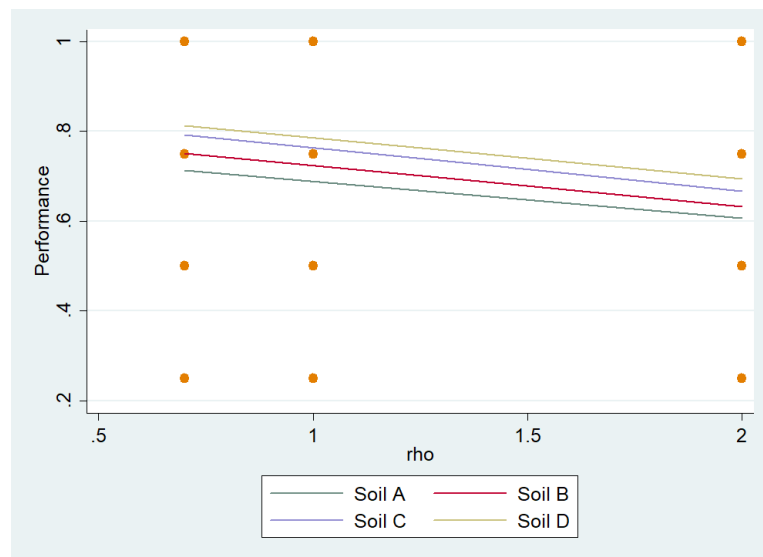
Figure 3.3. Scatter plot of ρ vs. Performance

Figure 3.3 displays a more significant change in performance related to reinforcement ratio when compared to concrete compressive strength.

As mentioned in the preceding section, the difference between confined and unconfined sections in terms of ductility and energy dissipation capacity is significant. This can also be inferred from the drastic change in performance in Figure 3.4.
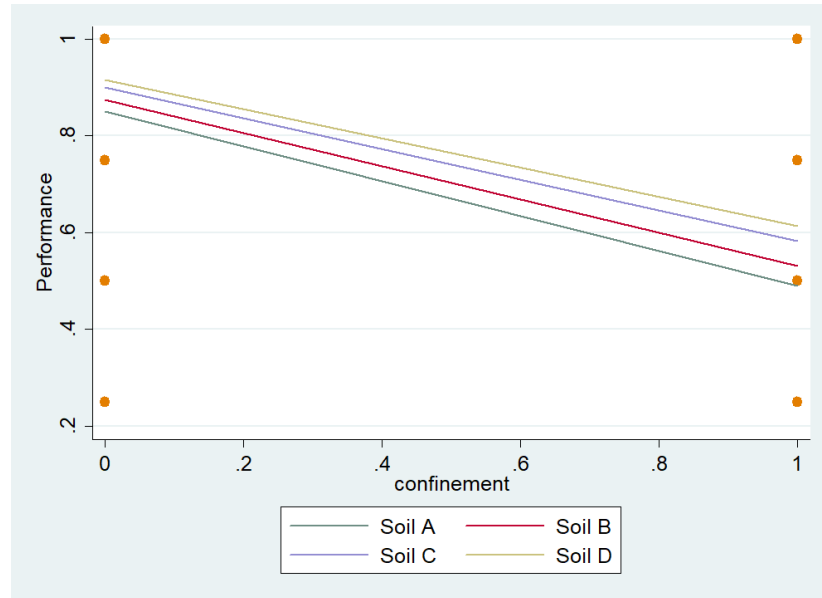
Figure 3.4. Scatter plot of Confinement vs. Performance
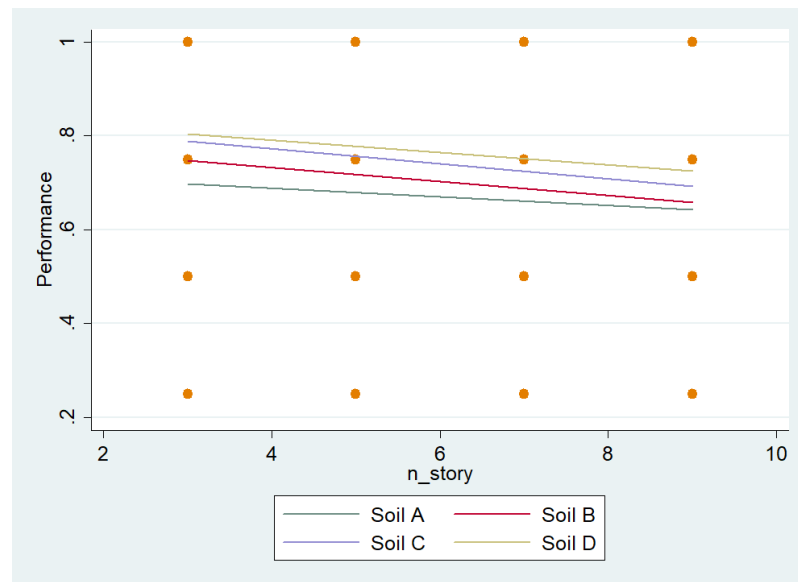
Figure 3.5. Scatter plot of n_story vs. Performance

Equation (2.16) implies that the energy spectra, which were calculated using mass-normalized values, are directly correlated with the total mass of a structure. Therefore, it would be reasonable to anticipate that performance would decline as mass increased. However, Figure 3.5 suggests the contrary. Even though the demand on a structure increases, structures perform better as the total height increases. This might be explained by the RC structures' redistribution property, which has to do with how energy is distributed throughout the structure during hinge propagation. It also might be attributed to the increase in capacity. Nevertheless, one cannot claim that simply increasing the number of stories will improve performance as there are many other parameters to consider. Figure 3.6 shows the anticipated rise in structural damage when soft story is present. Its impact is considerably less than one might expect. In order to better understand the impact of this parameter, the soft story's height may be increased.
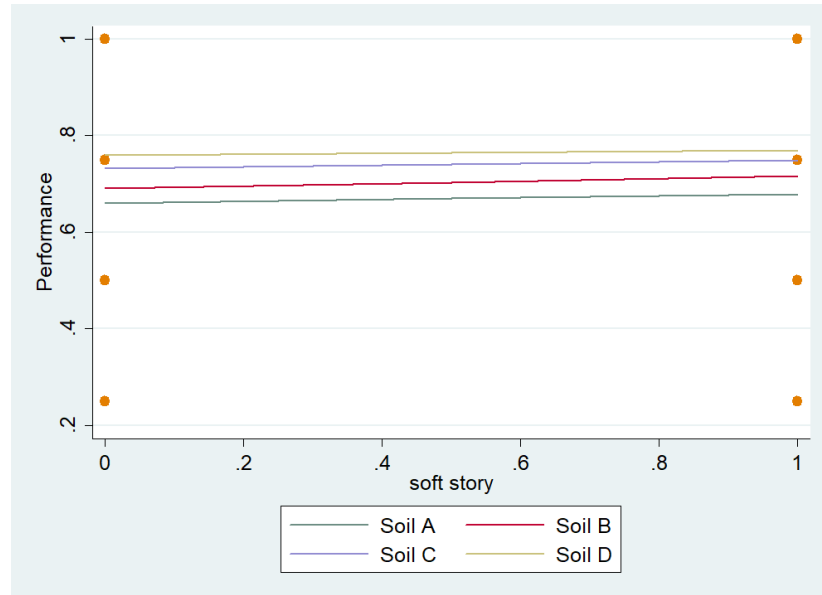
Figure 3.6. Scatter plot of Soft Story vs. Performance

In Dindar's plastic demand energy formula (see Equation (2.16)), the effect of PGA is shown to be quadratic. Its impact on demand energy and, subsequently, rising damage levels cannot be understated. Figure 3.7 makes this quite clear.
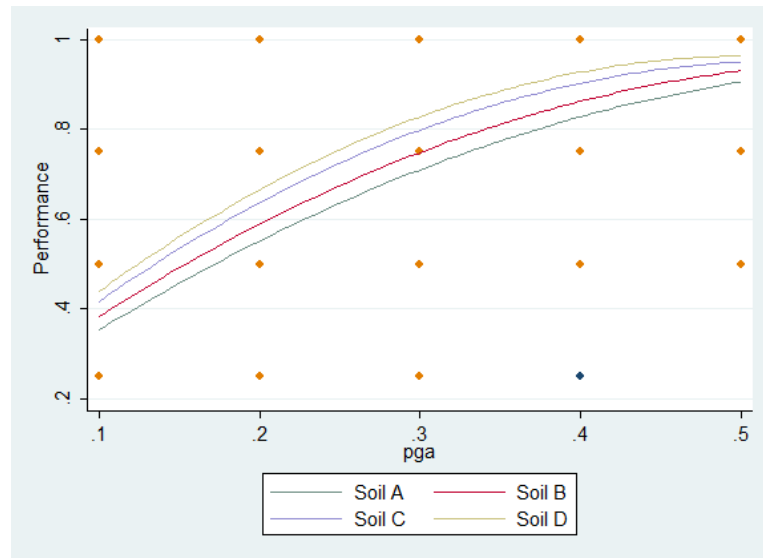
Figure 3.7. Scatter plot of PGA vs. Performance

It was put forth by Dindar *et al.* [16] that an increase in target ductility results in higher energy demand values for structures in a certain period range. In this range, the ratio of plastic energy to total input energy increases with ductility levels. However, for structures out of this category, the opposite is valid. The models used in this study clearly fall into the first category, as Figure 3.8 demonstrates.
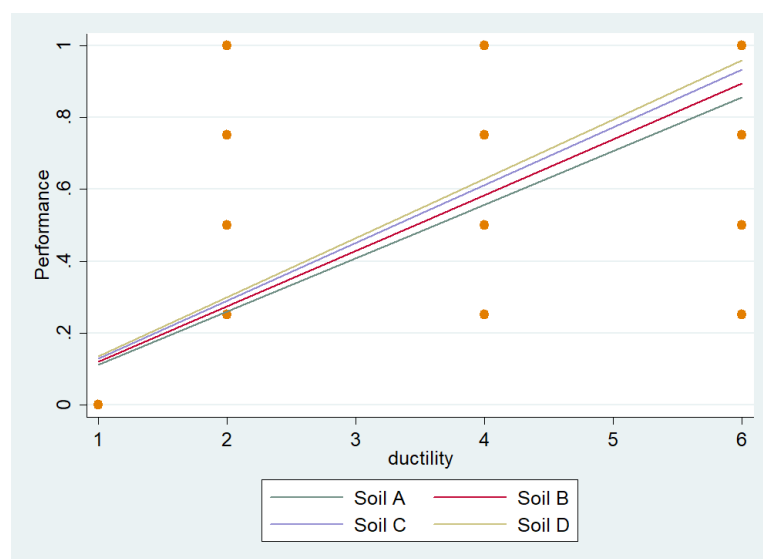
Figure 3.8. Scatter plot of Ductility vs. Performance

3.3. Statistical Analysis

In order to understand how specific aspects of the structures and scenarios impact the performance quantitatively, data from the parametric research was analyzed using statistical methods. STATA, a program for statistical analysis [48], was utilized for this.

This thesis has discussed the significant nonlinearities and various parameters that affect the performance of existing structures. Hence, using a few simple regression analyses to estimate a structure's performance cannot produce results that are accurate or comprehensive which can be inferred from the scatter plots in the preceding section. Consequently, a multivariate regression analysis was required to produce the performance function.

Considering the nonlinearity of parameters and their relation to the dependent variable, performance level, nonlinear regression models might be more accurate and flexible compared to linear models. However, estimating nonlinear models with numerous variables is a challenging task, in addition to increasing the complexity of the regression model, which contradicts the goal of creating a simple model for screening.

A linear multivariate regression model can be utilized as in the expression given in [49]. In this model r is the number of independent, or explanatory, variables and β_1 through β_r represent the coefficients for each independent variable whereas the constant of the model is denoted by β_0. ϵ is the error in this equation and the summation yields the dependent variable Y. The Ordinary Least Squares (OLS) method was utilized for the estimation of the linear relationship between the dependent and independent variables which can be described as

$$Y = \beta_0 + \beta_1 x_1 + \beta_2 x_2 + ... + \beta_r x_r + \epsilon. \tag{3.1}$$

The OLS multivariate regression analysis in STATA was conducted using the data from the parametric study. Practical outcomes were not obtained when soil type was included as a categorical variable. Therefore, it was decided to divide the data set into

four equal parts with respect to soil type and conduct four separate analyses. The program outputs for each analysis are given in Figures 3.10 through 3.13.

All regression analyses demonstrate good correlation between the parameters and the performance levels. This stems from the fact that the data set was created through numerical and analytical analyses using these parameters. P values (see $P > |t|$ columns) being extremely close to zero for each parameter in each analysis is the main indicator of how statistically significant these parameters are for performance.

A measure of how well the regression model fits the data set is R-squared value. It is calculated using the ratio of sum squares of residuals to total sum of squares. It could also be described as the percentage of the dependent variable's variation. Hence, the higher the R-squared value, the better the model fits the data. All regression analyses produced R-squared values high enough for the models to be reliable. A better fit in the model could be seen for soil type A when compared to the others. An R-squared value around 70 % proves a good fitted model for regression [50].

```
. reg perf n_bay

      Source |       SS           df       MS            Number of obs =     240
-------------+----------------------------------        F(  1,    238) =    0.16
       Model |  .01171875         1    .01171875        Prob > F       =  0.6941
    Residual |  17.9880208       238    .075579919       R-squared      =  0.0007
-------------+----------------------------------        Adj R-squared  = -0.0035
       Total |  17.9997396       239    .075312718       Root MSE       =  .27492

-------------------------------------------------------------------------------
        perf |      Coef.   Std. Err.      t    P>|t|     [95% Conf. Interval]
-------------+-----------------------------------------------------------------
       n_bay |     .00625   .0158724     0.39   0.694    -.0250183    .0375183
       _cons |   .6020833   .0583189    10.32   0.000     .4871961    .7169705
-------------------------------------------------------------------------------
```

Figure 3.9. STATA simple regression output for number of bays.

As mentioned in part 3.1.1, the number of bays was not taken as a parameter in this study since it did not prove to be an important factor in the determination of performance levels. 4 buildings having the same properties, except for the number of bays they have, were analyzed for 60 cases each. A simple regression analysis was

conducted based on the 240 performance levels obtained from this small study. The P value, showing the increase in significance of a parameter for a data set as it gets close to 0, turned out to be very high. Also, the R-squared value turned out to be very low. Therefore, the inclusion of the number of bays as a parameter would not have a significant effect on performance. The output of the simple regression is given in Figure 3.9.

In the models created as a result of the regression analyses, coefficients (given in the first column of the bottom tables) reveal how a one unit increase in the parameters changes the dependent variable. Therefore, if the coefficient of a variable is positive, the dependent variable increases as that particular variable increases while others remain constant, and vice versa if it is negative. All analyses result in negative coefficients for number of stories, f_{ck}, reinforcement ratio, and confinement, whereas positive coefficients for soft story, ductility, and PGA. These findings have good correlation with the scatter plots and fitted curves presented in the previous section. The coefficients for each parameter should be evaluated while keeping the units used in this study under consideration (i.e., MPa, g).

```
. reg performance n_story fck rho confinement softstory ductility pga if soil==1
```

Source	SS	df	MS		
Model	161.831558	7	23.118794		
Residual	42.3348485	2152	.019672327		
Total	204.166406	2159	.094565265		

Number of obs = 2160
F(7, 2152) = 1175.19
Prob > F = 0.0000
R-squared = 0.7926
Adj R-squared = 0.7920
Root MSE = .14026

performance	Coef.	Std. Err.	t	P>|t|	[95% Conf. Interval]	
n_story	-.0092361	.0013496	-6.84	0.000	-.0118828	-.0065894
fck	-.0032986	.000616	-5.35	0.000	-.0045067	-.0020906
rho	-.0811601	.00543	-14.95	0.000	-.0918087	-.0705115
confinement	-.3604167	.0060357	-59.71	0.000	-.3722532	-.3485802
softstory	.0196759	.0060357	3.26	0.001	.0078394	.0315124
ductility	.0231771	.0018481	12.54	0.000	.0195529	.0268013
pga	1.381944	.0213396	64.76	0.000	1.340096	1.423793
_cons	.534565	.0175429	30.47	0.000	.5001621	.5689679

Figure 3.10. STATA regression output for soil type A

```
. reg performance n_story fck rho confinement softstory ductility pga if soil==2

      Source |       SS       df       MS              Number of obs =    2160
-------------+------------------------------           F(  7,  2152) = 1063.51
       Model |  155.493066      7  22.2132951           Prob > F      =  0.0000
    Residual |  44.9483404   2152  .020886775           R-squared     =  0.7758
-------------+------------------------------           Adj R-squared =  0.7750
       Total |  200.441406   2159  .092839929           Root MSE      =  .14452

-------------+----------------------------------------------------------------
 performance |      Coef.   Std. Err.      t    P>|t|     [95% Conf. Interval]
-------------+----------------------------------------------------------------
     n_story |  -.0146528   .0013907   -10.54   0.000    -.01738    -.0119256
         fck |  -.0025174   .0006348    -3.97   0.000    -.0037621   -.0012726
         rho |  -.0910147   .0055951   -16.27   0.000    -.101987   -.0800423
 confinement |   -.343287   .0062193   -55.20   0.000    -.3554834   -.3310906
    softstory |   .0256944   .0062193     4.13   0.000     .0134981    .0378908
    ductility |   .0210069   .0019043    11.03   0.000     .0172726    .0247413
         pga |   1.367477   .0219884    62.19   0.000     1.324356    1.410598
       _cons |   .6030616   .0180763    33.36   0.000     .5676127    .6385105
-------------+----------------------------------------------------------------
```

Figure 3.11. STATA regression output for soil type B

```
. reg performance n_story fck rho confinement softstory ductility pga if soil==3

      Source |       SS       df       MS              Number of obs =    2160
-------------+------------------------------           F(  7,  2152) =  922.20
       Model |  141.996164      7  20.2851662           Prob > F      =  0.0000
    Residual |  47.3367066   2152  .021996611           R-squared     =  0.7500
-------------+------------------------------           Adj R-squared =  0.7492
       Total |   189.33287   2159  .087694706           Root MSE      =  .14831

-------------+----------------------------------------------------------------
 performance |      Coef.   Std. Err.      t    P>|t|     [95% Conf. Interval]
-------------+----------------------------------------------------------------
     n_story |  -.0159722   .0014271   -11.19   0.000    -.0187709   -.0131735
         fck |  -.0019676   .0006514    -3.02   0.003    -.003245   -.0006902
         rho |  -.0961731   .0057418   -16.75   0.000    -.1074332   -.084913
 confinement |  -.3180556   .0063824   -49.83   0.000    -.3305718   -.3055393
    softstory |   .0166667   .0063824     2.61   0.009     .0041504    .0291829
    ductility |   .0153646   .0019542     7.86   0.000     .0115323    .0191969
         pga |   1.332755    .022565    59.06   0.000     1.288503    1.377006
       _cons |   .6726065   .0185504    36.26   0.000     .636228     .708985
-------------+----------------------------------------------------------------
```

Figure 3.12. STATA regression output for soil type C

```
. reg performance n_story fck rho confinement softstory ductility pga if soil==4
```

Source	SS	df	MS
Model	132.240543	7	18.8915061
Residual	50.035383	2152	.023250643
Total	182.275926	2159	.084426089

Number of obs =	2160
F(7, 2152) =	812.52
Prob > F =	0.0000
R-squared =	0.7255
Adj R-squared =	0.7246
Root MSE =	.15248

performance	Coef.	Std. Err.	t	P>|t|	[95% Conf. Interval]	
n_story	-.0134259	.0014673	-9.15	0.000	-.0163033	-.0105485
fck	-.0011285	.0006697	-1.69	0.092	-.0024418	.0001849
rho	-.0911521	.0059032	-15.44	0.000	-.1027287	-.0795755
confinement	-.3027778	.0065618	-46.14	0.000	-.3156458	-.2899097
softstory	.0087963	.0065618	1.34	0.180	-.0040718	.0216644
ductility	.0121528	.0020091	6.05	0.000	.0082128	.0160928
pga	1.311343	.0231993	56.52	0.000	1.265847	1.356838
_cons	.6785667	.0190718	35.58	0.000	.6411656	.7159678

Figure 3.13. STATA regression output for soil type D

Following observations could be made from the regression analysis results:

- Coefficient associated with confinement has a great impact on the performance for all soil types. Increasing confinement from 0 to 1 while keeping everything else constant reduces the dependent variable by 0.36, 0.34, 0.32 and 0.30 for soil types A, B, C and D, respectively. This demonstrates that confinement is more important for soil type A, almost by 20% compared to soil D, 12.5% compared to soil C, and 6% compared to soil B. Given that the performance levels are spaced out at intervals of 0.25, by looking at the coefficient for confinement, it could be inferred that the presence of confinement changes the performance level of a structure on its own. However, the assumption that the value 0 for confinement refers to completely unconfined sections must be noted.

- As f_{ck} increases by 1 MPa, the damage decreases by 0.0033 for soil type A. Going from 8 to 20 MPa, it decreases by 0.0400 in total. This value is smaller for soils B, C, and D. Therefore, it is not enough to change the performance level by itself.

- Comparing the maximum and minimum number of stories, 3 and 9, the damage difference between the two is 0.0958 for soil type C and it is lower for other soil

types. The damage level gets lower as the number of stories increases.

- As ρ increases by 1% , the damage decreases by 0.0812 for soil type A. Going from 0.7 to 2%, it decreases by 0.100 in total. This value is larger for soils B, C and D. Even though it is not enough to change the performance level alone, it makes a great impact.

- Presence of soft story has the ability of changing the damage by 0.0256 for soil type B and it is even smaller for other soil types. Hence, the effect of soft story is minimal for the structures in this study. Judging from its P value, the presence of story for soil type D is much less significant compared to other parameters.

- Increasing ductility from 2 to 6 increases the damage by 0.0927 for soil type A which can be considered significant even though is not enough to change the performance level by itself.

- PGA levels were proven to be crucial for the performance level determination by these analyses. Increasing PGA from 0.1 to 0.5 g s increases the damage by 0.5245 for soil type D. This corresponds to more than two intervals of performance. This value is even bigger for other soil types.

- The constant value of the regression model gets bigger as the soil type changes from A to D and it is essential to the model since the corresponding P value is very small.

3.4. Screening Method Procedure

This method's primary objective is to evaluate the performance of existing residential structures that have specific deficiencies. Energy-Based numerical analyses were utilized to produce a data set that represented a variety of scenarios and the performance levels related to them. A polynomial equation with each term describing a characteristic of the structure to be evaluated was produced by statistical analysis of this data set. Therefore, this method does not require a structural analysis. The only parameter that needs to be predefined or estimated is the target ductility level which could be taken between 2.5 and 3.0.

Based on the regression analyses described in the previous section, a damage model was created for the screening method. The formulation of the damage model is expressed as

$$D = \beta_1 x_1 + \beta_2 x_2 + \beta_3 x_3 + \beta_4 x_4 + \beta_5 x_5 + \beta_6 x_6 + \beta_7 x_7 + C, \qquad (3.2)$$

where D, β_i, and x_i represent the damage score, the coefficients and real values of the variables, respectively. The dependent variable D is indexed between 0 and 1 and specifies the performance level of the structure in question. Table 3.3 displays the parameters, coefficients, and the symbols associated with them.

Table 3.3. Regression model coefficients and symbols.

Parameters	Symbols	Coefficients			
		Soil A	Soil B	Soil C	Soil D
n_story	β_1	-0.0093	-0.0147	-0.0160	-0.0134
f_{ck} (MPa)	β_2	-0.0033	-0.0025	-0.0020	-0.0011
ρ (%)	β_3	-0.0812	-0.0910	-0.0962	-0.0911
Confinement (0-1)	β_4	-0.3604	-0.3433	-0.3181	-0.3028
Soft Story (0,1)	β_5	0.0200	0.0257	0.0167	0.0088
Ductility	β_6	0.0232	0.0210	0.0154	0.0122
PGA (g)	β_7	1.3819	1.3675	1.3328	1.3113
Constant	C	0.5346	0.6031	0.6726	0.6786

Table 3.4 displays the performance zones based on damage score. Damage scores associated with each performance level ranged from 0.25 to 1.0. Due to the lack of zero values the performance zones had to be adjusted to fit the model.

Table 3.4. Performance zones based on damage score.

Performance level	LD	CD	CP	CO
Damage Score	0-0.375	0.376-0.625	0.626-0.875	0.876-1

Steps of the proposed screening method can be listed as:

(i) The application range of the screening method is governed by the scope of the techniques employed to produce the damage function. Determining whether the structure in question is covered by the approach is first step. The scope is detailed in this section.

(ii) Determination of demand parameters:

   (a) PGA value from Seismic Hazard Map.

   (b) Soil Type.

   (c) Target ductility level: There are various approaches for determining this parameter. Force reduction factors recommended in Table 4.1 of TSC 2018 [22] may be used to determine target ductility levels. The table defines 3 categories of cast in-situ RC buildings in terms of their ductility capacity: highly ductile, mixed ductility, and limited ductility. The relation between the force reduction factor and ductility is given in TSC 2018 [22] as

$$\frac{R}{I} = \mu D, \tag{3.3}$$

   where R is force reduction factor, μ is ductility, I is building importance factor, and D is coefficient of excess strength. I is taken as 1 for residential structures and D is given in Table 4.1 of TSC 2018 [22]. Considering the structures that fall into the scope of this study, according to the method given by TSC [22], target ductility level varies between 3.2 and 2. To be on the safe side, a value between 2.5 and 3.0 could be used.

(iii) Determination of structural parameters:

   (a) Number of stories.

   (b) Presence of soft story.

   (c) Compressive strength of the concrete, f_{ck}.

   (d) Average longitudinal reinforcement ratio.

   (e) Confinement level: Assumet to be a binary variable in this study, hence, requires the evaluation of the engineer.

(iv) Acquisition of the regression model coefficients from Table 3.3 based on Soil Type.

(v) Calculation of the damage score D using the regression model.

(vi) Determination of the performance level based on the performance zones given in Table 3.4.

(vii) Since the structural deficiencies included in this model are limited, the final score might require to be modified by the engineer.

3.4.1. Interpretation of the Screening Results

According to the guidelines listed in the Turkish Seismic Code [22], structures at the Limited Damage (LD) and Controlled Damage (CD) levels should be retrofitted, while structures at the Collapse Prevention (CP) and Collapse (CO) levels are considered to be dangerous in terms of life safety.

If a structure is deemed to be at the Collapse Prevention (CP) or Collapse (CO) levels by the model described above, the structure must be investigated in detail as soon as possible. Nonlinear evaluation methods described in TSC 2018 [22] are recommended.

The regression models proposed in this thesis fail to adequately simulate the effect of soft story. The reduction in performance is much less than expected when compared to other studies. For instance, the PERA method proposed by Ilki *et al.* [51] assigns a penalty score of 0.85 to the overall performance when soft story is present. For the structures with damage scores close to the limits of the performance levels, a 15% increase in damage could prove crucial. The structures at the Controlled Damage (CD) level with soft story defects must be further investigated. It would not be safe to continue operating these buildings without taking any strengthening measures.

3.4.2. Examples

Four random frame models were taken from the data set to evaluate using the regression model. These models and their parameters are given in Table 3.5 where n_s,

n_b, C and SS correspond to number of stories, number of bays, confinement and soft story, respectively. The ductility level here was assumed to be input by the user. The rightmost column depicts the outputs of the MATLAB program for these cases.

Table 3.5. Example cases to be evaluated.

Cases	n_s	n_b	f_{ck}	ρ	C	SS	μ	PGA	Soil	Perf.
Case 1	3	4	14	0.7	1	0	2	0.3	1	"CD"
Case 2	5	4	20	2	1	0	2	0.1	4	"LD"
Case 3	7	4	20	0.7	0	1	6	0.3	1	"CO"
Case 4	9	4	8	2	1	1	4	0.5	2	"CP"
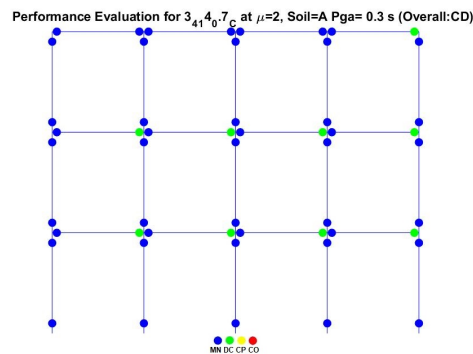
(a) Output for the Case 1.
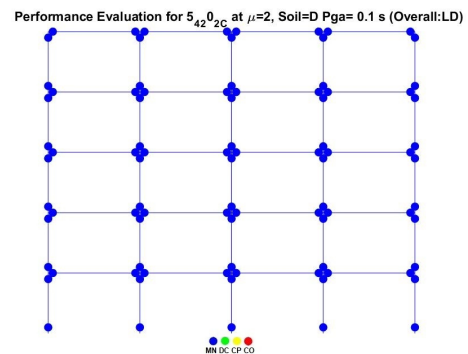
(b) Output for the Case 2.
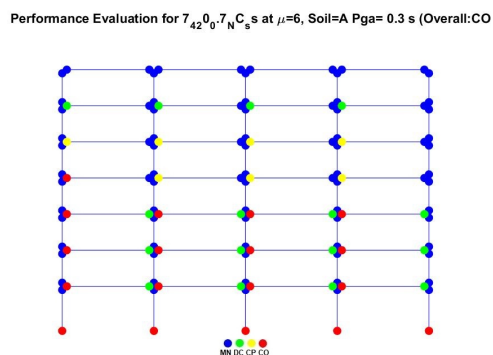
(c) Output for the Case 3.
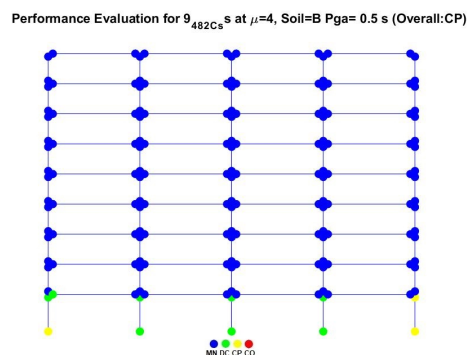
(d) Output for the Case 4.

Figure 3.14. Outputs of the performance module of the MATLAB program for the example cases.

The outputs of the performance module of the MATLAB program for the above cases are given in Figure 3.14. Damage propagation at hinges can be seen in the color coded scheme.

Using the coefficients given in Table 3.3, the regression equation for case 1 can be written as

$$D_1 = -0.0093 \times 3 - 0.0033 \times 14 - 0.0812 \times 0.7 - 0.3604 \times 1$$
$$+0.0200 \times 0 + 0.0232 \times 2 + 1.3819 \times 0.3 + 0.5346 = 0.5043.$$

(3.4)

The regression equation for case 2 can be written as

$$D_2 = -0.0134 \times 5 - 0.0011 \times 20 - 0.0911 \times 2 - 0.3028 \times 1$$
$$+0.0088 \times 0 + 0.0122 \times 2 + 1.3113 \times 0.1 + 0.6786 = 0.2592.$$

(3.5)

The regression equation for case 3 can be written as

$$D_3 = -0.0093 \times 7 - 0.0033 \times 20 - 0.0812 \times 0.7 - 0.3604 \times 0$$
$$+0.0200 \times 1 + 0.0232 \times 6 + 1.3819 \times 0.3 + 0.5346 = 0.9203.$$

(3.6)

The regression equation for case 4 can be written as

$$D_4 = -0.0147 \times 9 - 0.0025 \times 8 - 0.0910 \times 2 - 0.3433 \times 1$$
$$+0.0257 \times 1 + 0.0210 \times 4 + 1.3675 \times 0.5 + 0.6031 = 0.7192.$$

(3.7)

Using the results of these equations, the performance levels were determined in accordance with the zones described in Table 3.4. The results were compared in Table 3.6 with the MATLAB program outputs. Very good correlation between the estimated values and program outputs can be observed.

Table 3.6. Comparison of the outputs of MATLAB and regression model.

Frame Name	Perf. (Model)	Perf. (MATLAB)
Case 1	"CD"	"CD"
Case 2	"LD"	"LD"
Case 3	"CO"	"CO"
Case 4	"CP"	"CP"

4. SUMMARY AND CONCLUSIONS

4.1. Summary

The performance evaluation of existing residential buildings is critical to minimizing life loss as a result of a potential earthquake. Given the high volume of structures in urban areas, researchers devised a number of rapid seismic screening methods, some of which found acceptance in seismic codes. These methods primarily rely on the two most well-known approaches as a foundation: Force and Displacement-Based approaches. A third approach for the design and evaluation of structures was introduced in the 1980's: the Energy-Based approach. This approach distinguishes itself from prior techniques by using earthquake duration, frequency content, and energy dissipation capacity as factors. Therefore, by developing a rapid seismic screening method based on Energy-Based principles, the accuracy could be improved. The Energy-Based Design algorithm proposed by Yalçın *et al.* [1] was utilized in this study for the purpose of developing such a method. A MATLAB program that executes their algorithm with the help of three external programs, XTRACT, SAP2000 and IDARC2D, was developed. SAP2000 was mainly used for the determination of demand distribution through the frame for different ductility levels, whereas IDARC2D was used for the determination of energy dissipation capacity and damage levels occurring on a structure during cyclic motion. The guidelines in the Turkish Seismic Code for the determination of performance levels were also integrated into this code.

A parametric study on the performance levels of structures considering parameters concrete compressive strength, reinforcement ratio, confinement, presence of soft story, ductility, PGA, and soil type was conducted using the MATLAB program. 144 frame models were created and 8640 data points were obtained, which were then analyzed statistically using the software STATA. Finally, a regression model for each soil type was created for the purpose of predicting the performance level of existing residential buildings.

4.2. Conclusions

The following conclusions could be drawn from the findings of the study described in this thesis:

- In the parametric study, soil type D produced the highest damage values, and soil type A produced the lowest damage values. These findings could be used to observe the impact of soil type on earthquake energy demand.

- Given the large coefficients of ductility (0.01795 on average) and PGA (1.3484 on average) in the regression model, the significance of energy imparted into the structure on performance is evident. Therefore, it is imperative to define the structure accurately so that the model reflects key characteristics.

- One of the most crucial characteristics in this investigation was the presence of confinement in sections. Confinement impacts not just energy dissipation capacity but also demand by influencing the period through behavior.

- The increase in the number of stories, concrete quality, reinforcement ratio, and confinement level reduces the damage, while the increase in ductility and PGA increases the damage. PGA, ductility, confinement and confinement were proven to be very sensitive parameters.

- The soft story effect was found to be less substantial than expected. Even though the soft story columns would have more energy dissipation capacity, due to increase in length, compared to other floor columns, the energy demand should have accumulated more on the floor with soft story, reducing its performance. The reason why this was not observed could be linked to how the frame models were defined. The definition of diaphragms and constraints could be revisited to solve this problem so that the interstory drift for soft story is much higher.

- Dindar's predicted increase in plastic energy demand [9] for intermediate period values could be seen in the results.

- The R-squared values used to determine the method's validity in relation to the data came out to be between 72.5% and 79.2%. These numbers could be considered as satisfactory but achieving higher values is possible by considering

other parameters to determine performance level.

- An approximate interval for target ductility was suggested. A ductility level between 2.5 and 3.0 could be used in the rapid screening procedure. The engineer's judgment is very important at this point.

4.3. Future Work

The Energy-Based Design approaches presented and used in this thesis open many possibilities for improving the seismic assessment of RC structures. The following enhancements can be made to this study and other energy-related seismic research:

- The Energy-Based Design methodology proposed by Yalçın *et al.* [1] is only applicable for low-to-mid rise moment resisting frames. Moreover, the effect of shear walls and infill walls are excluded from the analyses. The researchers [1] anticipate that the methodology's application could be expanded to cover 3D frames or frames with shear walls. The seismic screening method proposed in this thesis could also be updated accordingly.

- Extending the data set used to create the regression models could significantly improve the accuracy. This could only be possible by lowering the analysis run times. As mentioned in the preceding chapters, SAP2000 API has certain limitations that increase the run time. Other structural analysis software can be used to execute the MATLAB code. Furthermore, including a Graphical User Interface would improve the code's functionality.

- The addition of more structural features and defects is necessary to reflect more real-life structures and broaden the application of the screening procedure. For example, to close the gap between the two confinement levels employed in this study, lateral reinforcement ratio could be incorporated into the code. The effects of short columns, torsional irregularities and vertical irregularities could also be included.

- The regression model proposed in this thesis could be improved by modifying the relationship between the parameters and their coefficients based on the assessment

of real life structures.

- The application of data mining approaches may yield new insights into the relationship between the dependent and independent variables employed in statistical analysis. The use of decision trees or artificial intelligence (AI) could introduce a new process for assessing structures.

REFERENCES

1. Yalçın, C., A. A. Dindar, E. Yüksel, H. Özkaynak and O. Büyüköztürk, "Seismic Design of RC Frame Structures Based on Energy-Balance Method", *Engineering Structures*, Vol. 237, p. 112220, 2021.

2. Priestley, M., "Performance Based Seismic Design", *Bulletin of the New Zealand Society for Earthquake Engineering*, Vol. 33, No. 3, pp. 325–346, 2000.

3. Newmark, N. M. and W. J. Hall, *Earthquake Spectra and Design*, Earthquake Engineering Research Institute, California, 1982.

4. Priestley, M. N., "Myths and Fallacies in Earthquake Engineering: Conflicts Between Design and Reality", *Bulletin of the New Zealand Society for Earthquake Engineering*, Vol. 26, No. 3, pp. 329–341, 1993.

5. Lam, N., J. Wilson and G. Hutchinson, "The Ductility Reduction Factor in the Seismic Design of Buildings", *Earthquake Engineering & Structural Dynamics*, Vol. 27, No. 7, pp. 749–769, 1998.

6. Chopra, A. K., *Dynamics of Structures: Theory and Applications to Earthquake Engineering*, Prentice Hall, New Jersey, 1995.

7. Priestley, M., G. Calvi and M. Kowalsky, "Direct Displacement-Based Seismic Design of Structures", *New Zealand Society for Earthquake Engineering Conference*, 2007.

8. Priestley, M. and G. Calvi, "Concepts and Procedures for Direct Displacement-Based Design and Assessment", *Seismic Design Methodologies for the Next Generation of Codes*, Vol. 1, No. 16, pp. 171–181, 1997.

9. Dindar, A. A., *Energy-Based Earthquake Response Analysis and Design of Rein-*

forced Concrete SDOF Columns, Ph.D. Thesis, Boğaziçi University, 2009.

10. Housner, G. W., "Limit Design of Structures to Resist Earthquakes", *The First World Conference on Earthquake Engineering*, 1956.

11. Zahrah, T. F. and W. J. Hall, "Earthquake Energy Absorption in SDOF Structures", *Journal of Structural Engineering*, Vol. 110, No. 8, pp. 1757–1772, 1984.

12. Akiyama, H., *Earthquake-Resistant Limit-State Design for Buildings*, University of Tokyo Press, Tokyo, 1985.

13. Akbaş, B., *Energy-Based Earthquake Resistant Design of Steel Moment Resisting Frames*, Ph.D. Thesis, University of Illinois at Urbana-Champaign, 1997.

14. Shen, J. and B. Akbaş, "Seismic Energy Demand in Steel Moment Frames", *Journal of Earthquake Engineering*, Vol. 3, No. 04, pp. 519–559, 1999.

15. Ye, L., G. Cheng and Z. Qu, "Study on Energy-Based Seismic Design Method and Application on Steel Braced Frame Structures", *Jianzhu Jiegou Xuebao Journal of Building Structures*, Vol. 33, No. 11, pp. 36–45, 2009.

16. Dindar, A. A., C. Yalçın, E. Yüksel, H. Özkaynak and O. Büyüköztürk, "Development of Earthquake Energy Demand Spectra", *Earthquake Spectra*, Vol. 31, No. 3, pp. 1667–1689, 2015.

17. Özdemir, U., *Development of Quick Seismic Evaluation Methodology for the Existing Reinforced Concrete Buildings*, Master's Thesis, Boğaziçi University, 2003.

18. Ozcebe, G., M. Yucemen, V. Aydogan and A. Yakut, "Preliminary Seismic Vulnerability Assessment of Existing Reinforced Concrete Buildings in Turkey Part 1", *Seismic Assessment and Rehabilitation of Existing Buildings*, Vol. 1, No. 1, pp. 29–42, 2003.

19. Yakut, A., V. Aydogan, G. Ozcebe and M. Yucemen, "Preliminary Seismic Vulnerability Assessment of Existing Reinforced Concrete Buildings in Turkey Part 2", *Seismic Assessment and Rehabilitation of Existing Buildings*, Vol. 1, No. 1, pp. 43–58, 2003.

20. Tezcan, S. S., I. E. Bal and F. G. Gulay, "P25 Scoring Method for the Collapse Vulnerability Assessment of R/C Buildings", *Journal of the Chinese Institute of Engineers*, Vol. 34, No. 6, pp. 769–781, 2011.

21. Bertero, V. V. and A. Terán Gilmore, "Use of Energy Concepts in Earthquake-Resistant Analysis and Design: Issues and Future Directions", *Memorias: Seminario Latinoamericano de Ingeniería Sismo Resistente, 8 y Primeras Jornadas Andinas de Ingeniería Estructural*, Vol. 1, No. 1, pp. 1–39, 1993.

22. "Turkish Earthquake Design Code Specification for Structures to be Built in Seismic Areas", Disaster and Emergency Management Presidency, Ankara, 2018.

23. Uang, C.-M. and V. V. Bertero, "Evaluation of Seismic Energy in Structures", *Earthquake Engineering & Structural Dynamics*, Vol. 19, No. 1, pp. 77–90, 1990.

24. Mahin, S. A. and V. V. Bertero, "An Evaluation of Inelastic Seismic Design Spectra", *Journal of the Structural Division*, Vol. 107, No. 9, pp. 1777–1795, 1981.

25. Kunnath, S. and Y. Chai, "Cumulative Damage-Based Inelastic Cyclic Demand Spectrum", *Earthquake Engineering & Structural Dynamics*, Vol. 33, No. 4, pp. 499–520, 2004.

26. Decanini, L. D. and F. Mollaioli, "An Energy-Based Methodology for the Assessment of Seismic Demand", *Soil Dynamics and Earthquake Engineering*, Vol. 21, No. 2, pp. 113–137, 2001.

27. Kuwamura, H. and T. V. Galambos, "Earthquake Load for Structural Reliability", *Journal of Structural Engineering*, Vol. 115, No. 6, pp. 1446–1462, 1989.

28. Chou, C.-C. and C.-M. Uang, "A Procedure for Evaluating Seismic Energy Demand of Framed Structures", *Earthquake Engineering & Structural Dynamics*, Vol. 32, No. 2, pp. 229–244, 2003.

29. Güllü, A., E. Yüksel, C. Yalçın, A. Anıl Dindar, H. Özkaynak and O. Büyüköztürk, "An Improved Input Energy Spectrum Verified by the Shake Table Tests", *Earthquake Engineering & Structural Dynamics*, Vol. 48, No. 1, pp. 27–45, 2019.

30. Acun, B. and H. Sucuoğlu, "Energy Dissipation Capacity of Reinforced Concrete Columns under Cyclic Displacements.", *ACI Structural Journal*, Vol. 109, No. 4, pp. 531–540, 2012.

31. Erberik, A. and H. Sucuoğlu, "Seismic Energy Dissipation in Deteriorating Systems Through Low-Cycle Fatigue", *Earthquake Engineering & Structural Dynamics*, Vol. 33, No. 1, pp. 49–67, 2004.

32. "Turkish Earthquake Design Code Specification for Structures to be Built in Seismic Areas", Disaster and Emergency Management Presidency, Ankara, 2007.

33. El-Bahy, A., S. K. Kunnath, W. C. Stone, A. W. Taylor *et al.*, "Cumulative Seismic Damage of Circular Bridge Columns: Benchmark and Low-Cycle Fatigue Tests", *ACI Structural Journal*, Vol. 96, pp. 633–641, 1999.

34. Park, Y.-J. and A. H.-S. Ang, "Mechanistic Seismic Damage Model for Reinforced Concrete", *Journal of Structural Engineering*, Vol. 111, No. 4, pp. 722–739, 1985.

35. "MATLAB Version 9.5.0 (R2018b) Manual", The MathWorks Inc., Natick, MA, 2018.

36. "SAP2000: Integrated Software for Structural Analysis & Design Version 23.0.0. Manual", Computers and Structures Inc., Berkeley, CA, 2021.

37. "ASCE 41-13: Seismic Evaluation and Upgrade of Existing Buildings", American

Society of Civil Engineers, Reston, 2013.

38. Merter, O. and T. Ucar, "Design of RC frames for Pre-selected Collapse Mechanism and Target Displacement Using Energy–Balance", *Sadhana*, Vol. 39, No. 3, pp. 637–657, 2014.

39. Reinhorn, A., H. Roh, M. Sivaselvan, S. Kunnath, R. Valles, A. Madan and Y. Park, "IDARC2D Version 7.0: A Program for the Inelastic Damage Analysis of Structures", *Multidisciplinary Center for Earthquake Engineering Research*, Vol. 1, pp. 15–242, 2009.

40. Sürmeli, M., *Performance Evaluation of Precast Columns Under Seismic Excitation*, Master's Thesis, Istanbul Technical University, 2008.

41. "XTRACT-Cross Section Analysis Program for Structural Engineers Version 3.0.3", Imbsen Software Systems, Sacramento, CA, 2004.

42. "FEMA 356", US Federal Emergency Management Agency, Washington, DC, 2000.

43. Pinto, P. E. and P. Franchin, "Eurocode 8-Part 3: Assessment and Retrofitting of Buildings", *Proceedings of the Eurocode*, Vol. 8, pp. 10–11, 2011.

44. Saatcioglu, M. and S. R. Razvi, "Strength and Ductility of Confined Concrete", *Journal of Structural Engineering*, Vol. 118, No. 6, pp. 1590–1607, 1992.

45. Sheikh, S. A. and S. Uzumeri, "Analytical Model for Concrete Confinement in Tied Columns", *Journal of the Structural Division*, Vol. 108, No. 12, pp. 2703–2722, 1982.

46. Mander, J., M. Priestley and R. Park, "Observed Stress-Strain Behavior of Confined Concrete", *Journal of Structural Engineering*, Vol. 114, No. 8, pp. 1827–1849, 1988.

47. AFAD, "Türkiye Deprem Tehlike Haritası", 2019, `https://deprem.afad.gov.tr/deprem-tehlike-haritasi`, accessed on July 12, 2022.

48. "Stata Data Analysis and Statistical Software Special Edition Release", StataCorp, 2007.

49. Johnson, R. A., I. Miller and J. E. Freund, *Probability and Statistics for Engineers*, Pearson Education, London, 2000.

50. Nau, R., "Statistical Forecasting: Notes on Regression and Time Series Analysis", 2009, `https://people.duke.edu/ rnau/411home.htm`, accessed on July 22, 2022.

51. Ilki, A., M. Comert, C. Demir, K. Orakcal, D. Ulugtekin, M. Tapan and N. Kumbasar, "Performance Based Rapid Seismic Assessment Method (PERA) for Reinforced Concrete Frame Buildings", *Advances in Structural Engineering*, Vol. 17, No. 3, pp. 439–459, 2014.

APPENDIX A: SAMPLED OUTPUTS OF THE PARAMETRIC STUDY

Table A.1. Sampled Outputs of the Parametric Study.

n_s	f_{ck} (MPa)	ρ (%)	Conf.	SS	μ	PGA (g)	Soil	Perf.
3	14	0.7	1	0	6	0.1	1	0.25
5	20	1	1	0	6	0.5	3	1
5	8	0.7	1	0	4	0.1	2	0.25
9	14	0.7	0	1	6	0.4	1	1
5	8	0.7	1	0	6	0.4	4	1
3	8	1	0	0	4	0.3	4	1
7	14	0.7	1	1	2	0.1	2	0.25
3	14	1	0	0	4	0.4	1	1
3	14	0.7	1	1	2	0.5	1	1
7	8	2	0	0	6	0.3	1	1
7	8	0.7	0	0	2	0.3	4	1
7	20	1	0	1	2	0.3	4	1
5	20	1	1	0	6	0.3	3	0.75
5	20	0.7	1	0	4	0.1	2	0.25
5	8	1	1	0	4	0.2	3	0.5
5	20	1	0	1	6	0.4	2	1
3	8	2	0	1	4	0.1	3	0.75
3	14	1	1	0	6	0.4	4	1
5	20	2	0	0	6	0.5	2	1
3	14	2	1	0	4	0.4	3	0.5
7	20	2	0	0	6	0.1	2	0.25
7	14	2	0	1	2	0.1	3	0.25
5	8	1	0	1	2	0.1	2	0.5
5	8	2	1	0	2	0.1	4	0.25

Table A.1. Sampled Outputs of the Parametric Study. (cont.)

n_s	f_{ck} (MPa)	ρ (%)	Conf.	SS	µ	PGA (g)	Soil	Perf.
5	8	0.7	1	1	4	0.3	2	0.5
9	8	1	0	0	6	0.3	2	1
9	14	1	0	0	2	0.2	2	0.5
3	20	1	1	0	4	0.5	4	1
5	20	0.7	1	1	4	0.4	2	0.75
5	20	2	1	0	6	0.1	2	0.25
7	14	2	0	0	2	0.4	1	1
9	8	1	0	1	2	0.3	2	1
9	14	1	0	0	4	0.3	4	1
7	8	0.7	0	1	6	0.2	3	1
9	14	1	0	0	4	0.4	1	1
5	8	2	1	1	2	0.3	4	0.5
3	14	2	0	1	4	0.4	1	1
7	20	1	0	0	4	0.4	2	1
5	20	0.7	1	0	6	0.1	1	0.25
7	20	2	0	1	6	0.3	1	1
7	8	0.7	0	0	2	0.2	3	1
9	8	1	0	0	4	0.1	2	0.5
5	8	0.7	0	0	6	0.1	3	0.75
9	20	1	0	0	4	0.2	4	1
7	20	1	1	1	2	0.5	4	1
9	14	2	1	0	2	0.3	1	0.5
7	20	2	1	0	6	0.2	2	0.25
5	20	2	1	1	4	0.2	4	0.5
3	20	1	1	0	6	0.3	4	0.75
5	20	1	0	1	6	0.5	1	1
9	20	2	1	0	2	0.2	2	0.25

Table A.1. Sampled Outputs of the Parametric Study. (cont.)

n_s	f_{ck} (MPa)	ρ (%)	Conf.	SS	μ	PGA (g)	Soil	Perf.
5	8	2	1	0	4	0.5	3	0.75
3	20	0.7	0	1	6	0.3	1	1
9	14	2	0	0	6	0.4	1	1
5	8	0.7	1	1	4	0.1	3	0.25
9	20	1	0	1	6	0.3	2	1
3	8	2	1	0	2	0.4	1	0.5
7	8	2	0	1	6	0.3	1	1
9	20	2	0	0	2	0.2	3	0.5
3	14	2	1	1	4	0.2	4	0.25
3	8	2	0	0	2	0.5	4	1
5	20	2	0	1	6	0.5	3	1
7	8	1	0	1	6	0.1	1	0.5
5	8	0.7	0	1	4	0.4	4	1
5	14	1	1	1	6	0.3	1	0.5
3	20	0.7	1	0	4	0.5	2	1
5	20	0.7	0	1	2	0.2	4	1
5	8	0.7	1	0	6	0.1	2	0.25
3	14	1	1	0	6	0.1	1	0.25
5	14	0.7	1	0	4	0.1	1	0.25
7	14	2	0	1	4	0.1	2	0.25
9	20	2	0	0	6	0.1	3	0.25
7	20	2	0	1	2	0.2	1	0.5
7	14	0.7	0	1	2	0.1	4	0.5
9	8	0.7	1	1	6	0.1	2	0.25
5	20	0.7	0	0	6	0.1	4	0.75
3	14	2	0	1	2	0.4	3	1
3	14	1	0	1	2	0.3	4	1

Table A.1. Sampled Outputs of the Parametric Study. (cont.)

n_s	f_{ck} (MPa)	ρ (%)	Conf.	SS	µ	PGA (g)	Soil	Perf.
9	20	1	1	0	2	0.1	3	0.25
9	14	0.7	1	0	6	0.2	3	0.25
3	14	0.7	1	0	2	0.5	3	1
5	14	2	0	1	4	0.4	3	1
9	8	2	0	1	2	0.5	1	1
5	8	0.7	1	0	4	0.4	4	1
3	20	2	1	0	2	0.5	2	0.75
7	20	0.7	0	1	4	0.2	1	0.75
7	20	0.7	0	0	2	0.5	1	1
5	14	2	0	1	4	0.5	4	1
3	8	0.7	1	0	2	0.3	3	1
5	14	2	1	0	4	0.4	4	0.75
3	14	0.7	0	1	2	0.2	1	0.75
9	8	2	0	0	6	0.4	2	1
3	20	1	0	1	2	0.4	4	1
9	14	0.7	0	0	6	0.4	4	1
9	20	0.7	1	1	6	0.4	4	1
9	8	0.7	1	0	2	0.4	4	1
9	14	2	0	1	6	0.3	4	1
7	8	1	1	1	4	0.1	4	0.25
5	14	0.7	0	0	6	0.4	3	1
5	20	1	0	1	2	0.1	4	0.5
5	20	0.7	1	1	2	0.3	1	0.25
7	8	0.7	1	1	2	0.2	4	0.5
3	8	2	0	0	2	0.3	1	1
3	8	2	1	0	2	0.3	1	0.25
5	14	0.7	0	1	6	0.2	2	1

Table A.1. Sampled Outputs of the Parametric Study. (cont.)

n_s	f_{ck} (MPa)	ρ (%)	Conf.	SS	μ	PGA (g)	Soil	Perf.
9	20	0.7	0	1	2	0.5	2	1
5	20	1	1	0	6	0.3	4	1
9	14	2	0	1	4	0.3	4	1
5	14	1	1	1	4	0.1	4	0.25
9	8	1	0	0	6	0.5	3	1
7	20	1	1	0	6	0.1	4	0.25
5	8	1	1	1	4	0.5	4	1
7	14	0.7	1	0	4	0.4	1	0.75
7	8	2	1	0	4	0.5	2	0.5
3	8	1	0	1	2	0.1	2	0.5
3	14	2	0	0	4	0.1	2	0.75
7	14	0.7	1	1	2	0.5	3	1
7	20	1	0	0	6	0.1	3	0.5
5	8	0.7	0	0	6	0.1	2	0.75
9	14	2	1	1	6	0.3	2	0.5
3	20	0.7	1	0	2	0.4	3	1
7	14	1	0	1	4	0.4	2	1
9	20	1	1	0	2	0.3	2	0.5
9	8	2	0	1	4	0.3	3	1
9	8	0.7	0	0	6	0.5	4	1
9	20	1	1	1	4	0.3	4	0.5
3	14	1	0	0	4	0.1	4	0.75
5	20	1	0	0	6	0.4	4	1
9	8	1	1	0	6	0.3	2	0.5
9	14	0.7	1	1	4	0.3	2	0.5
9	14	0.7	1	0	4	0.3	4	0.5
5	20	0.7	0	1	6	0.2	3	1

Table A.1. Sampled Outputs of the Parametric Study. (cont.)

n_s	f_{ck} (MPa)	ρ (%)	Conf.	SS	µ	PGA (g)	Soil	Perf.
3	8	1	1	1	4	0.4	1	0.5
7	8	0.7	1	0	4	0.5	4	1
3	14	2	1	0	2	0.5	2	0.5
9	14	2	1	1	2	0.3	2	0.5
3	20	1	0	0	2	0.3	2	1
9	8	0.7	0	1	6	0.3	1	1
5	14	2	0	1	2	0.1	4	0.5
7	20	1	1	0	2	0.3	4	0.75
7	8	1	0	0	4	0.2	1	0.75
5	14	2	1	1	4	0.2	3	0.25

APPENDIX B: COPYRIGHT PERMISSIONS FOR FIGURES

Development of Earthquake Energy Demand Spectra

Author: Ahmet Anıl Dindar, Cem Yalçın, Ercan Yüksel, et al
Publication: Earthquake Spectra
Publisher: SAGE Publications
Date: 08/01/2015

Copyright © 2015, © SAGE Publications

Gratis Reuse

Permission is granted at no cost for use of content in a Master's Thesis and/or Doctoral Dissertation, subject to the following limitations. You may use a single excerpt or up to 3 figures tables. If you use more than those limits, or intend to distribute or sell your Master's Thesis/Doctoral Dissertation to the general public through print or website publication, please return to the previous page and select 'Republish in a Book/Journal' or 'Post on intranet/password-protected website' to complete your request.

BACK

CLOSE WINDOW

Figure B.1. Copyright permission for Figure 2.4.

CCC | Marketplace™

Order Date	05-Sep-2022	Type of Use	Republish in a thesis/dissertation
Order License ID	1265160-1	Publisher	JOHN/WILEY & SONS LTD.
ISSN	0098-8847	Portion	Image/photo/illustration

LICENSED CONTENT

Publication Title	Earthquake engineering & structural dynamics	Rightsholder	John Wiley & Sons - Books
		Publication Type	Journal
Article Title	An improved input energy spectrum verified by the shake table tests	Start Page	27
		End Page	45
Author/Editor	INTERNATIONAL ASSOCIATION FOR EARTHQUAKE ENGINEERI	Issue	1
Date	01/01/1972	Volume	48
Language	English		
Country	United Kingdom of Great Britain and Northern Ireland		

REQUEST DETAILS

Portion Type	Image/photo/illustration	Distribution	Other territories and/or countries
Number of images / photos / illustrations	1	Enter territories/countries	Turkey
Format (select all that apply)	Print, Electronic	Translation	Original language of publication
Who will republish the content?	Academic institution	Copies for the disabled?	No
Duration of Use	Life of current edition	Minor editing privileges?	No
Lifetime Unit Quantity	Up to 499	Incidental promotional use?	No
Rights Requested	Main product	Currency	USD

NEW WORK DETAILS

Title	RAPID SEISMIC SCREENING OF REINFORCED CONCRETE BUILDINGS USING ENERGY-BASED PRINCIPLES	Institution name	Bogazici University
		Expected presentation date	2022-09-09
Instructor name	Cem Yalçın		

ADDITIONAL DETAILS

The requesting person / organization to appear on the license	Ahmet Mehdi Darılmaz

REUSE CONTENT DETAILS

Title, description or numeric reference of the portion(s)	Figure 10	Title of the article/chapter the portion is from	An improved input energy spectrum verified by the shake table tests
Editor of portion(s)	Anıl Dindar, A.; Büyüköztürk, Oral; Güllü, Ahmet; Yalçın, Cem; Yüksel, Ercan; Özkaynak, Hasan	Author of portion(s)	Anıl Dindar, A.; Büyüköztürk, Oral; Güllü, Ahmet; Yalçın, Cem; Yüksel, Ercan; Özkaynak, Hasan
Volume of serial or monograph	48	Publication date of portion	2019-01-01
Page or page range of portion	27-45		

Figure B.2. Copyright permission for Figure 2.5.

CCC | Marketplace™

This is a License Agreement between Ahmet Mehdi Darılmaz ("User") and Copyright Clearance Center, Inc. ("CCC") on behalf of the Rightsholder identified in the order details below.
The license consists of the order details, the Marketplace Order General Terms and Conditions below, and any Rightsholder Terms and Conditions which are included below.
All payments must be made in full to CCC in accordance with the Marketplace Order General Terms and Conditions below.

Order Date	05-Sep-2022	Type of Use	Republish in a thesis/dissertation
Order License ID	1265102-1	Publisher	PERGAMON
ISSN	0141-0296	Portion	Image/photo/illustration

LICENSED CONTENT

Publication Title	Engineering structures	Rightsholder	Elsevier Science & Technology Journals
Article Title	Seismic design of RC frame structures based on energy-balance method	Publication Type	Journal
Date	01/01/1978	Start Page	112220
Language	English	Volume	237
Country	United Kingdom of Great Britain and Northern Ireland		

REQUEST DETAILS

Portion Type	Image/photo/illustration	Distribution	Other territories and/or countries
Number of images / photos / illustrations	3	Enter territories/countries	Turkey
Format (select all that apply)	Print, Electronic	Translation	Original language of publication
Who will republish the content?	Academic institution	Copies for the disabled?	No
Duration of Use	Life of current edition	Minor editing privileges?	No
Lifetime Unit Quantity	Up to 499	Incidental promotional use?	No
Rights Requested	Main product	Currency	USD

NEW WORK DETAILS

Title	RAPID SEISMIC SCREENING OF REINFORCED CONCRETE BUILDINGS USING ENERGY-BASED PRINCIPLES	Institution name	Bogazici University
		Expected presentation date	2022-09-09
Instructor name	Cem Yalçın		

ADDITIONAL DETAILS

Order reference number	N/A	The requesting person / organization to appear on the license	Ahmet Mehdi Darılmaz

REUSE CONTENT DETAILS

Title, description or numeric reference of the portion(s)	Figure 1, Figure 2, Figure 3	Title of the article/chapter the portion is from	Seismic design of RC frame structures based on energy-balance method
Editor of portion(s)	Yalçın, Cem; Dindar, Ahmet Anıl; Yüksel, Ercan; Özkaynak, Hasan; Büyüköztürk, Oral	Author of portion(s)	Yalçın, Cem; Dindar, Ahmet Anıl; Yüksel, Ercan; Özkaynak, Hasan; Büyüköztürk, Oral
Volume of serial or monograph	237	Issue, if republishing an article from a serial	N/A
Page or page range of portion	112220	Publication date of portion	2021-06-15

Figure B.3. Copyright permissions for Figure 2.6, Figure 2.7, Figure 2.8.

To Boğaziçi University Institute of Graduate Studies in Science and Engineering

I grant permission for the reuse of Figure 3.14 and Figure 3.15 from my Master's thesis (Surmeli,2008) in Ahmet Mehdi Darılmaz's Master's thesis.

Melih

Figure B.4. Copyright permission for Figure 2.13.